

INVESTIGATION OF PHARMACEUTICAL DRUGS AND MEDICINES
BY LASER-INDUCED PLASMA (BREAKDOWN) SPECTROSCOPY

A THESIS SUBMITTED TO

THE GRADUATE SCHOOL OF NATURAL AND APPLIED SCIENCES

OF

ATILIM UNIVERSITY

BY

NASER FARHAT ALMSELLATI

IN PARTIAL FULFILLMENT OF THE REQUIREMENTS FOR THE DEGREE

OF

DOCTOR OF PHILOSOPHY

IN

MODELING AND DESIGN OF ENGINEERING SYSTEMS (MODES)

(MAIN FIELD of STUDY: PHYSICS)

JAN 2018

Approval of the Graduate School of Natural and Applied Sciences, Atılım University

Prof. Dr. Ali Kara
Director

I certify that this thesis satisfies all the requirements as a thesis for the degree of
doctor of philosophy

Assoc. Prof. Dr. Ender Keskinliç
Head of Department

This is to certify that we have read the thesis “investigation of pharmaceutical drugs and medicines by laser-induced plasma (breakdown) spectroscopy” submitted by “Candidates Name: Naser Farhat Almsellati” and that in our opinion; it is fully adequate, in scope and quality, as a thesis for the degree of doctor of philosophy.

Assoc. Prof. Dr. Kemal Efe Eseller
Co-Supervisor

Prof. Dr. Ramazan Aydın
Supervisor

Examining Committee Members

Prof. Dr. Ramazan Aydın

Assoc. Prof. Dr. Burak Yedierler

Assoc. Prof. Dr. Filiz Özkan

Assoc. Prof. Dr. Halil Berberoğlu

Assoc. Prof. Dr. Reşat Ö. Doruk

Date: Jan. 04.01.2018

I declare and guarantee that all data, knowledge and information in this document has been obtained, processed, and presented in accordance with academic rules and ethical conduct. Based on these rules and conduct, I have fully cited and referenced all material and results that are not original to this work.

Name, Last name: NASER FARHAT ALMSELLATI

Signature:

ABSTRACT

INVESTIGATION OF PHARMACEUTICAL DRUGS AND MEDICINES BY LASER-INDUCED PLASMA (BREAKDOWN) SPECTROSCOPY

NASER FARHAT ALMSELLATI

Ph.D. Modeling and Design of Engineering Systems (Physics)

Supervisor: Prof. Dr. Ramazan Aydin

Co-Supervisor: Assoc. Prof. Dr. Kemal Efe Eseller

Jan 2018, 72 pages

Laser-induced Breakdown Spectroscopy (LIBS), which is a laser based diagnostic technique, which is effective to test concentrations various solids, liquids and gases. It's laser-induced breakdown plasma comprises of electrons, and ionic/neutral particles. Neutral and ionized atoms release optical emissions, which help obtaining emission spectrum, which requires analysis. The LIBS spectrum analysis identifies those elements, which are present in a sample and it gives information regarding elemental concentrations in a test medium.

This study aims to develop a laser-induced breakdown spectroscopic method to improve the detection limits of the pharmaceutical samples. The study will start with analysis on current techniques. The well-known experimental techniques will also be compared in terms of various accuracy characteristics for measuring different parameters. In conclusion, a new model will be elaborated with respect to pharmaceutical industry based on laser and spectrographic types, and also the limitations on detection capability.

Keywords: laser, break down spectroscopy, plasma, electron density and signal-to-noise ratio.

ÖZ

İLAÇ VE UYUŞTURUCU TIBBİ MADDELERİN İÇERİKLERİNİN

LAZER UYARMALI PLAZMA ANALİZ SPEKTROSKOPİSİ

TEKNİĞİ İLE ARAŞTIRILMASI

NASER FARHAT ALMSELLATI

Doktora, Mühendislik Sistemlerinin Modellenmesi ve Tasarımı Anabilim Dalı
(Fizik)

Tez Yöneticisi: Prof. Dr. Ramazan Aydın

Ortak Tez Yöneticisi: Doç. Dr. Kemal Efe Eseller

Ocak 2018, 72 sayfa

Lazerle uyarılan plazma spektroskopisi, katı, sıvı ve gazlarda element konsantrasyonunun ölçülmesinde başarıyla kullanılmaktadır. Lazerle oluşturulan plazma elektron ve iyonların yanı sıra nötr parçacıklardan oluşmaktadır. Bu ölçüm tekniğinde nötr ve iyonlardan gelen emisyon spektrumu kaydedilir ve bu spektrumu analiz edilerek içinde var olan elementler tanımlanır ve bunların test madde içindeki konsantrasyonları belirlenir.

Bu çalışmada, ilaç ve benzeri tıbbi maddelerin içeriklerini mevcut araştırma yöntemlerine göre daha duyarlı ve kesin biçimde elde etmek amacıyla, lazerle oluşturulan plazma spektroskopisi analiz edildi. Bu deney tekniği ve elde edilen bulgular literatürde yer alan benzeri deney sonuçları ve kuramsal çalışmalar ile karşılaştırıldı.

Sonuç olarak, bu çalışmada geliştirilen ölçüm tekniği, gerek lazer özellikleri gerekse incelenen numunelerin içerdiği elementleri belirleme duyarlılığı bakımından üstünlüklere sahip olduğu saptandı.

Anahtar Kelimeler: Lazer, plazma, çökme plazma spektroskopisi, elektron yoğunluğu ve sinyal gürültüsü oranı.

To My Parents and My Family

ACKNOWLEDGMENTS

Primarily, I thank Allah and I Praise Him for giving me the opportunity to complete this work.

I express sincere appreciation to my supervisor Prof. Dr. Ramazan Aydin and Assoc. Prof. Dr. Kemal Efe Eseller for their valuable support, advice, guidance, suggestions and help throughout the research.

Also, I would like to thank the staff of the Department of Physics of Atılım University and Middle East Technical University for their efforts to help the students to provide support for gaining knowledge.

Finally, I would like to thank my family, friends, and everyone, who helped me during the study.

Table of Contents

INVESTIGATION OF PHARMACEUTICAL DRUGS AND MEDICINES BY LASER-INDUCED PLASMA (BREAKDOWN) SPECTROSCOPY	1
CHAPTER 1	1
INTRODUCTION	1
CHAPTER 2	4
THEORETICAL APPROACH.....	4
2.1 Introduction to Laser Spectroscopy.....	4
2.1.1 Absorption Spectroscopy	4
2.1.2 Emission Spectroscopy	6
2.2 Spectral Line Broadening Effects.....	6
2.2.1 Natural Line Broadening.....	7
2.2.2 Doppler Broadening	8
2.2.3 Pressure Broadening	8
2.2.4 Stark Broadening.....	8
2.3 The Fundamental Properties of Plasma.....	9
CHAPTER 3	16
ATOMIC EMISSION SPECTROSCOPY.....	16
3.1 Introduction	16
3.2 Radiation from Atoms	16
3.3 ElectricDipoleTransition Selection Rules	17
3.4 Forbidden Transitions.....	16
3.5 Oscillator Strength.....	18
3.6 Intensities of spectral lines	18
3.7 Continuous Emission and Bremsstrahlung.....	19

3.8	Broadening of Spectral Lines	20
3.9	Temperature and Equilibrium	21
CHAPTER 4		22
EXPERIMENTAL TECHNIQUE		22
4.1	Introduction	22
4.2	Laser-induced Breakdown Spectroscopy	22
4.3	Some Applications of LIBS	24
4.4	Overview of the Experimental LIBS	24
4.4.1	Principles of the Experimental Method	24
4.4.2	Laser as Light Source	25
4.4.3	Excitation by Laser Light	25
4.4.4	The Fibre Optical Cable.....	26
4.4.5	Advantages.....	27
4.4.6	The Detectors	27
4.4.7	Broadband Diode Array Spectrometers	27
4.4.8	Echelle Spectrometers.....	28
4.4.9	Czerny-Turner Spectrometers	28
4.5	Photomultiplier Tube (PMT)-Based Spectrometers	28
4.6	Pharmaceutical Applications.....	29
	Blend Uniformity	29
	Film Coating.....	29
4.7	Investigation and classification of Pharmaceutical Tablets.	29
4.7.1	Detection of Elements Distribution in Drugs.....	30
4.7.2	Classification.....	30
4.7.3	Cluster Analysis (CA).....	30
4.7.4	Clustering algorithms.....	30
4.8	Principle component analysis (PCA)	31

4.9	Artificial Neural Networks (ANNs)	31
4.10	SIMCA	33
4.11.	LIBS instrumentation.....	33
4.12	Experimental Procedure and Recording of Emission Spectra.....	33
CHAPTER 5		35
EXPERIMENTAL METHODS AND DATA ANALYZES.....		35
5.1	Introduction	37
5.2	Some General PCA Guidelines	38
5.3	PCA and Classification	38
5.4	VARIANCE AND GOAL.....	39
5.5	Principal Component Analysis.....	39
5.5.1	What is a Principal Component?.....	40
5.5.2	Characteristics of Principal Components.....	41
CHAPTER 6		43
PREDEFINED PCA PLOTS		43
6.1	PCA Overview	43
6.1.1	Scores.....	43
6.1.2	Finding Groups in a Scores Plot	44
6.1.3	Studying Sample Distribution in Scores Plot.....	44
6.1.4	Calibration and Validation Scores	45
6.1.5	Detecting outliers in a scores plot.....	45
6.2	The Figures Representative	46
6.2.1	X-variables correlation structure.....	47
6.3	Correlation Loadings Emphasize Variable Correlations.....	48
6.4	Influence Plot	49
6.5	Explained/Residual Variance	52

CHAPTER 7	55
7.3 Signals to Noise Ratio	55
7.4 Spectral Analysis.....	57
7.6 Loadings	61
7.6.1 X-variables correlation structure.....	61
7.7 Software Analysis.....	62
7.8 Correlation and variance analysis.....	62
CONCLUSION.....	66

LIST OF TABLE

TABLE 7.1 DETAILS OF INVESTIGATED PHARMACEUTICAL SAMPLES	36
TABLE 7. 2 DIFFERENT PEAKS OBSERVED IN THE LIBS SPECTRA AND THEIR CORRESPONDING ATOMIC ELEMENTS.	58
TABLE 7. 3 OXYGEN TO NITROGEN RATIOS WITH THE OXYGEN PEAK AT 777 NM (O) AND NITROGEN PEAKS AT 742.36 NM (N1) AND 744.23 NM (N2).	60

LIST OF FIGURES

FIGURE 3. 1 EMISSION AND ABSORPTION PROCESSES BETWEEN THE TWO ENERGY LEVELS.....	16
FIGURE 4. 1 OVERVIEW OF THE EXPERIMENTAL SET UP FOR LIBS	22
FIGURE 4. 2 ARTIFICIAL NEURAL NETWORKS	32
FIGURE 6. 1 TWO DIMENSIONS AND SCATTER PLOT OF SCORES.....	43
FIGURE 6. 2 FINDING GROUPS IN A SCORES PLOT	44
FIGURE 6. 3 SHOWS A SITUATION WITH FOUR DISTINCT CLUSTERS	45
FIGURE 6. 4 CALIBRATION AND VALIDATION	45
FIGURE 6.5 SAMPLES SHOWS AS OUTLIERS.....	46
FIGURE 6.6 SUBSTANTIAL PART OF VARIANCE OF X.....	47
FIGURE 6.7 LINE PLOT OF LOADINGS IN ASCENDING ORDER OF IMPORTANCE TO PC1 .	48
FIGURE 6.8 SHOW LOADING AND X-VARIABLES	48
FIGURE 6.9 CORRELATION LOADINGS EMPHASIZE VARIABLE CORRELATION.....	49
FIGURE 6.10CORRELATION LOADING	49
FIGURE 6.11 INFLUENCE PLOT.....	51
FIGURE 6.12 SHOWS DATA VARIATION.....	53
FIGURE6.13 SHOWS DATA VARIATION	53
FIGURE 6.14 SHOWS VARIANCES	54
FIGURE 7.1 THE PROPERTIES OF INTENSITY AND WAVELENGTH OF AFERIN TABLETS SHOW HYDROGEN 656 AND NITROGEN742. 744	35
FIGURE 7.2 THE PROPERTIES OF INTENSITY AND WAVELENGTH OF AFERIN TABLETS SHOW HYDROGEN 656 AND NITROGEN 742. 744 AND OXYGEN 777	36
FIGURE 7.3 EXPERIMENTAL SET UP	37
FIGURE 7.4 SHOWS SIGNALS TO NOISE RATIO OF K.....	55
FIGURE 7.5 SIGNAL TO NOISE RATIO GLUCOAMINE FOR NA	56
FIGURE 7.6 SIGNAL TO NOISE RATIO BRUFIN.....	56
FIGURE 7.7 SIGNAL TO NOISE RATIO GLUCOAMINE FOR NA.....	57

FIGURE 7.8 LIBS SPECTRA OF THE SAMPLES USED IN THE STUDY. (A) AFERIN, (B) PARAFON, (C) PAROL	57
FIGURE 7. 9 OXYGEN LIBS PEAKS FROM (A) AFERIN, (B) PARAFON, (C) PAROL. THE DOTS REPRESENT THE EXPERIMENTAL POINTS.....	59
FIGURE 7. 10 NITROGEN (N1 AND N2) LIBS PEAKS FROM (A) AFERIN, (B) PARAFON, (C) PAROL. THE DOTS REPRESENT THE EXPERIMENTAL POINTS	59
FIGURE 7. 11 SHOW THE POSITION OF H2 PEAKS FOR THE DIFFERENT TABLETS.	60
FIGURE7. 12SHOW THE DENSITY OF STATES OF DIFFERENT TABLETS.	61
FIGURE 7. 13 PCA GRAPH SHOWS TWO COMPONENTS PARAFON 300MG AND PAROL 650 MG	63
FIGURE 7. 14 PCA GRAPH SHOWS TWO COMPONENTS AFERIN 650 MG AND PARAFON 300MG	63
FIGURE 7. 15 PCA GRAPH SHOWS THREE COMPONENTS PAROL 500 MG.AFERIN 650 MG AND PARAFON 300MG.....	64
FIGURE 7. 16 PCA GRAPH SHOWS TWO COMPONENTS PAROL 500 MG AND AFERIN 650 MG.	64

LIST OF ABBREVIATIONS

LIBS	Laser-induced break down spectroscopy
PCA	Principle component analysis
LST	Long spark technique
TRE LIBS	Time Resolved Laser-induced break down spectroscopy
ICP	Inductively coupled plasma
AAS	Atomic absorption spectroscopy
AES	Atomic emission spectroscopy
AFS	Atomic fluorescence spectroscopy
CCD	Charge coupled device
PMT	Photo-Multiplier tube- based
SNR	Signal –to –noise -ratio
CA	Cluster analysis
ANNs	Artificial Neural Net works
SIMCA	Soft independent modelling by class analogy
IDA	Linear Discriminate Analysis
SVMC	Support vector machine classification

CHAPTER 1

INTRODUCTION

Laser-induced Breakdown Spectroscopy (LIBS) is an atomic emission spectroscopic technique, which was discovered after developments in laser technology in 1963. Laser plasma is generated and the intensities of the emission line are analyzed. In-situ and remote detection capability makes LIBS a preferable technique. LIBS plasma formation has been investigated since 1980's. Since that time, LIBS has become common for several analytical applications. In recent times, new technological developments of detectors, spectrographs and lasers were used. Q-switched laser technology has the ability to focus high power energy to create plasma. Analyzing new materials with the help of this new analytical tool makes LIBS a useful method. Atomization of the sample, excitations of the atoms, detection of emission, and calibration of intensity as a function of concentration are the main objectives in atomic emission spectroscopy. Plasma from a high-energy pulse laser is diverted on a single point, and resulting emissions are sent to the detection system with a proper fibre optic cable. Signal precision and accuracy can be obtained by averaging or pre-processing the data. The signal can be enhanced by increasing the signal-to-noise ratio (SNR) and eliminating interferences from continuum radiation.

LIBS were used initially for concentration measurements of solids, but nowadays it can be applied also to both gasses and liquids. Less energy is used to create atomization and the breakdown threshold, which is higher for gaseous samples. The LIBS signal can be detected under the surface of a liquid where the liquid is transparent at the laser wavelength. Double-pulse lasers can create significantly enhanced signals in liquids by creating a vapour-hollow space during the first pulse. Breakdown creates multi photon ionization at low pressure, and inverse Bremsstrahlung at high pressures from solids. The LIBS signal is produced by avalanche ionization. Recently LIBS was used to find the thickness of the coatings by applying several shots onto the surface of the coatings.

Laser spectroscopy is important for understanding and analyzing molecular and atomic compositions and energies. Technological developments in lasers, laser sources, such as pulse lasers, dye lasers, and tuneable lasers, have increased spectral resolution. A semi-classical approach to emission and absorption phenomena spectroscopic techniques help detecting sensitivity. We have studied LIBS to analyze the drug contents in tablet form (drugs and medicines), and investigated LIBS ability for routine classification of the tested elements as well.

This method is specifically helpful for quality control and assurance processes of pharmaceutical tablets. LIBS is actually atomic-emission spectroscopy that uses powerful laser for excitation and producing breakdown plasma [1]. The laser focus creates plasma that excites, atomizes or resolves the sample.

LIBS is a very helpful process that helps analyzing any element/matter irrespective of its physical form [2]. Since all the elements emit specific light with specific frequencies when treated at high energies, LIBS has the capacity to detect the elements present in any substance; however, the detection largely depends on intensity of laser, sensitivity and wavelength of spectrograph & detector [3]. If the material constituents are already unidentified, LIBS is still useful because it helps evaluating the proportion of every element or impurity. The previous studies reveal that other than carbon, hydrogen, nitrogen and oxygen, (active pharmaceutical ingredients) many inorganic elements are found in pharmaceutical tablets [4].

In detection/classification processes, chemo metric algorithms such as PCA (principal component analysis) and SIMCA (soft independent modelling of class analogy) were used to demonstrate that LIBS is capable of differentiating/ discriminating between medicine tablets [5].

LIBS normally needs little or no sample preparation and instrumentation, which is helpful to analyze industrial substances; therefore, it is a very useful tool [6].

LIBS signal is produced by avalanche ionization. Recently LIBS was used also to find the thickness of the coatings by applying several shots onto the surface of the coatings.

In brief, Q-switched laser can focus high power energy to create plasma. Analyzing new materials with this new analytical tool makes LIBS a useful method. Atomization

of the sample, excitations of the atoms, emission detection, and calibration of intensity are functions and main objectives of the under-discussion spectroscopy. As described briefly, plasma is focused using intense pulsed laser and the resulting emission is sent to the detection system through a proper fibre optic cable. Signal precision and accuracy are improved by taking averages of the studied units. The signal can be enhanced by increasing the signal-to-noise (SNR) and eliminating interferences from continuum radiation. It is used in express soil and mineral analysis (geology, mining, construction). Moreover, it is extensively used in almost all the material sciences, medical sciences, space science, earth sciences and manufacturing [1].

CHAPTER 2

THEORETICAL APPROACH

2.1 Introduction to Laser Spectroscopy

For atomic and molecular spectroscopy, laser has a unique light source (monochromatic, directional, coherent, single mode or multimode form, energetic etc) and it is the most commonly applied tool for excitation, ionization and other processes of spectroscopic investigations [7].

Laser helped introducing large number of new techniques and applications for conducting experiments. Many new optical changes are detectable using laser, and besides, researchers obtain voluminous spectroscopic data specifically pertaining to infrared spectral region. Researchers investigated intense laser beams and found several non-linear outcomes/effects.

Moreover, during the process, researchers found helpful spectroscopic data during researches on Raman spectra in all the forms of matter through spectra using laser as intense light source. Laser opened the possibility to eliminate Doppler broadening and at the same time, obtained resolutions that are comparable with the natural line width. These breakthroughs towards new experimental possibilities made laser spectroscopy more exciting than ever before.

Among the new laser radiation applications, laser-induced breakdown spectroscopy gained significance for analysing the constituents in materials. We'll discuss these techniques as well as properties of absorbing and emissive spectroscopy.

2.1.1 Absorption Spectroscopy

Laser beams are effective because they do not diverge much; that is directional, therefore, we can pass it through the sample repeatedly to maximize its absorption. Most of the absorption calculations are done in the spectral infrared area for investigating molecular transitions due to the rotation and the vibration effects. The rotational and vibration-rotation transitions take place in extremely large numbers to

correspond with molecular lasers, which are needed for measuring. Moreover laser transitions are recorded through scanning laser lines over the absorbing structure.

It is also possible that absorption line is moved through either the Zeeman or the Stark effect. To obtain better spectral line resolution, single-mode lasers are effective for scanning. Many investigations of spectroscopic absorption are conducted using tuneable lasers. On the other hand, pulsed lasers are used for operating new spectroscopic radiation sources. Measurement timing problems, environmental difficulties and spatial fluctuations while determining compositions have urged researchers to find more sensitive detection means. Improved detectors and spectroscopic techniques facilitate analysis even when signals are weak.

Laboratory conditions and techniques can generate new scope and applications for laser spectroscopy. The properties and production methods of single-mode lasers are excluded for clarity. In brief, the simplest tuneable laser applied for our purpose can be conventional gas laser operable with He-Ne, CO, or CO₂ lasers.

In spectral area, organic dye lasers are the most commonly used lasers. Laser spectroscopy with tuneable organic dye lasers is very helpful for chemical, physical or biological applications. As an example, concentration measurements, such as trace elements' existence within the chemical samples, are widely performed by making use of such lasers. Concentrations of chemical reactants or products and collision-induced energy transfer processes are best analyzed with the help of laser spectroscopic processes. Detection-sensitivity is the main concern for analytical chemists and researchers, especially when they initiate concentration measurements of impure molecules. Laser spectroscopic applications in absorption analysis generally require tuneable frequencies. Precision measurements with tuneable lasers are possible, for example, when two laser beams are passed through a sample in opposite directions so that the selective absorbing process can occur in atoms having zero-velocity. This helps eliminating the Doppler-broadening from spectral lines within the given specimen/sample.

Until the introduction of dye lasers, it was impossible to tune lasers selectively to multiple transitions in atoms and molecules, so, laser-guided spectroscopy brought precision and sensitivity of many orders. All those applications as well as calculations using tuneable and powerful lasers contributed to much better understanding and

interpretation of atomic and molecular processes [8]. In brief, absorption spectroscopy usually implies lasers of tuneable frequency.

2.1.2 Emission Spectroscopy

A simple technique for performing laser-spectroscopy is studying the spectrum of laser emission. Emission spectroscopy analyzes atomic and molecular emissions. By imposing any kind of energy, samples make transitions to lower lying levels by emitting electromagnetic radiation depending on energy levels. So, the emitted lines contain data including level structure, lifetime and excitation energy etc.

Using this process, many investigators collected the needed data pertaining to unknown energies and splitting [8]. They collected information pertaining to rotational and vibrating aspects of infrared lasers. They also conducted experiments on isotope-shift and their calculations through lasers having varying isotopes and measured their differences of wavelength.

Many results collected during the investigation of infrared noble gas lasers originated out of transition between Rydberg states with great principle quantum numbers. Wavelengths of these lines was calculated and measured, which is significant for the test of approximations for transition probabilities.

The accuracy of these experiments had limitations because of Doppler broadening. To reduce or remove such line broadenings, researchers used single-mode laser and tuneable category wherever possible. Both in the absorption and emission measurements as one of the important experimental uncertainties originate from the line broadenings of the spectral lines.

For reducing distortions/errors in calculations, the line widths of the transitions should be as narrow as possible. Line broadening takes place in atoms and molecules due to different factors, which are discussed in the following chapters.

2.2 Spectral Line Broadening Effects

Degeneration of electronic states, transition in oscillator strength, and excitation conditions determine spectral line intensities. The media, in which atoms exist, creates impact on radiating emissions. Thin medias prevent radiation re-absorption during the emission process. Emission out of optically allowed lower excited state into ground

state is called as resonance line and it gets affected from the self-absorption process at high concentrations, on which, line peaks are broadened and the amplitude is decreases.

2.2.1 Natural Line Broadening

Atoms decay from the excited states until the equilibrium in the atomic or molecular system is restored [9]. The rate of change has been given in the following equation:

$$\frac{dN_n}{dt} = A_{nm}N_n \quad (2.1)$$

Where N_n is the excited-state population number and A_{nm} is the Einstein's emission coefficient. Lifetime of n depends on the time of number of electrons dropping to 1/e. Heisenberg uncertainty relation concludes energy release and time-taken, which is measured along with the process and product of those relations, which must be bigger and equal plank constant.

Einstein emission coefficient can be defined as:

$$\mu_{x,y,z} = \sum_i q_i(x_i)_{x,y,z} \quad (2.2)$$

Selection rules determine transition probability $|R^{mn}|^2$:

$$R_{x,y,x}^{n,m} = \int \varphi_n^* \mu_{x,y,z} \varphi_m dx, dy, dz \quad (2.3)$$

$$|R^{n,m}|^2 = (R_x^{n,m})^2 + (R_y^{n,m})^2 + (R_z^{n,m})^2 \quad (2.4)$$

Here n has excited state while m has ground state. Both φ_n and φ_m are excited and ground state wave functions respectively. Einstein's emission coefficient can be presented as:

$$A_{n,m} = \frac{64\pi^4\nu^3}{(4\pi\epsilon_0)3hc^3} |R^{n,m}|^2 \quad (2.5)$$

Natural line broadening can be determined when Heisenberg uncertainty relation is put in the equation:

$$\Delta v \geq \frac{32\pi^3 v^3}{(4\pi\epsilon_0)3hc^3} |R^{n,m}|^2 \quad (2.6)$$

This type of broadening is in Lorentzian shape[10].

2.2.2 Doppler Broadening

When radiation emitted from moving atoms in media (e.g., in a gas or plasma) is detected in relation with the detector, broadening occurs[9]. Characteristic Doppler broadening is defined as:

$$\Delta v = \frac{v}{c} \left(\frac{2kT \ln 2}{m} \right)^{1/2} \quad (2.7)$$

Here " m " represents atomic mass and c shows the speed of light. In this case, broadening is higher than natural line-width while the line is in Gaussian shape. Measuring line-width helps identifying temperature of electrons, atoms and ions in media.

2.2.3 Pressure Broadening

Pressure broadening appears mostly in gaseous phase through direct collision process, which results in broadening energy of atoms. Broadening relation shows the dependency to average time of collision (Eq. 2.8).

$$\Delta v = (2\pi\tau)^{-1} \quad (2.8)$$

It is shown by Heisenberg's Uncertainty Principle that states that time and energy are not identifiable together. Pressure Broadening is in Lorentzian shape like naturally occurring line-width.

2.2.4 Stark Broadening

Interaction due to the electric field between species in medium is called Stark effect, which causes line broadening of transitions. The Stark broadening especially occurs in plasma conditions. Electron and ionic movement create electric field in plasma. The effects include atomic splitting/ shifting of atomic levels in an external electrical field.

Effects of electric fields (like plasma micro fields) are very significant on atomic levels for many atomic spectroscopic applications. That is why, besides quadratic and linear Stark effects, effects of inhomogeneous and variable fields need to be focused for precision measurements. Electric field acting on an atom creates Coulomb force. Spectral line-shift takes place, which splits the energy levels by certain frequency $\Delta\nu$ which, which is proportional with the electric field. Higher shift has quadratic Stark effects that make broadening asymmetric. Experiments identifying spectral line broadening are observable through several sources [5, 11].

2.3 The Fundamental Properties of Plasma

Matter exists in many forms, which depends on the physical environment. Conventional stable state classification includes three states including solid, liquid and gas; however, plasma is recognized as fourth state [9].

These states can transform into each other depending on temperature and energy. The plasma state establishes when gas ions/electrons are sufficient to dominate behaviour of the whole substance. Gases are different as compared to plasma because plasma conducts electricity while gases are insulators.

Atomic spectroscopy originated in mid-19th Century findings by Bunsen and Kirchhoff. They showed how optical radiation is a significant property of those elements, which can be traced in the flame-gases.

Experts have seen that the elemental intensities and spectra features such as existence of atomic spectral lines, and elemental species in a sample. We can say that in this context, both quantitative and qualitative analyses with atomic emission spectrometry and relevant options were fully explored. These discoveries took place with the help of prisms, which allowed radiation to disperse and produce the line spectra. The radiation should be spectrally handled. It was also found that radiation is different depending on the type of element.

This discovery, along with Fraunhofer's discovery that the solar radiation line spectrum has dark gaps, which takes place because of radiation absorption.

This observation set the grounds for atomic absorptive spectrometry. Flames are helpful for determining liquids. According to Bunsen and Kirchhoff, a link appeared

between atomic spectroscopy and the small element determination while very small quantities of elements laid the foundation for trace analyses. Industrial progress created great requirements for solid substance analysis.

Raw substances undergo large-scale processes for mass production, which add value to products. The need for suitable raw materials promoted mining, that took place on a large scale.

Geological analyses show that large samples of most of the elements experience low concentration levels the way it happens for noble materials.

There exists the requirement for not only raw materials characterization in bulk but process-controlled industrial production as well, and both of them introduced new demands. After the Second World War, it has been efficiently handled using atomic spectrometry and on the other hand, the information obtained pertaining to electrical discharge has promoted atomic spectrometric growth. Later, the importance of arc sparks was realized for the use of analyse ablation and solid materials' excitation.

In this way, it developed as a tool for semi-quantitative analyses while spark emission spectrometry is a decisively recommended procedure to conduct direct analytics. They are powerful radiation and laser sources [12].

Environment-friendly production processes are needed for reliable outcomes and elements/their variant forms. Limited flame temperatures might lead towards high temperature plasma.

The development of high-frequency and inductively-coupled plasma/ microwave plasma creates conveniences in the routine lab work. Atomic emission spectrometry is effective for multi-element analyses of all basic forms of matter. It takes place in various sources that are available but also for spectrometer design development.

The old spectroscopes were replaced by spectrographs having photographic detection, which was a major development after the investion of photoelectric multi-channel spectrometers. Nowadays array detectors are available. Lasers have given a new life to trace-analysis methodology.

They create newer forms of optical atomic spectrometry including laser-enhanced ionizing spectrometry. When intense laser output is diverted towards a gas, its intensity becomes equal to the critical threshold value that creates plasma.

Plasma looks like a bluish-white spark apparent with sharp sound. The occurrence of plasma is rare but it constituted 99% of all earthly and universal matter; therefore, it is significant for research.

Neutral matters turn into plasma through many ways but normally they absorb energy for generating ions and electrons. The system maintains neutral behaviour.

Where the number of electron (n_e) indicates electron density, " n_z " means density of ions of charge number z . Plasma emission spectrum is the outcome of many processes' effects.

Collisional, radioactive excitation, ionization, de-excitation, and recombination takes place using different energy levels. Many atomic processes act as inverse processes within thermodynamic systems. These processes, allow predicting an emission spectrum. Major processes occur within plasma, which are discussed below:

Collisional excitation uses an electron and a neutral particle or ion resulting in kinetic energy conversion into excitation energy. Conversely, collisional de-excitation converts to kinetic energy after collision. Collisional-ionization takes place when kinetic energy is enough to eliminate one more electron from an atom or molecule.

Collisional re-combination of an ion and an electron gain the kinetic energy. Photon excitation happens according to photon-absorption, which raises the system to a better state because it is converse of emission.

Photo-ionization occurs when there is enough energy profile for gaining an electron, which leads to higher ionization stage. During photo-recombination, electrons re-join ions through photoemission. Bremsstrahlung includes electron-ion encounter having ze charge; so both the particles have charge $(z-1)e$. A change towards lower continuum state might take place with the help of photon-emission through a process called as free-free transition. Conversely, in the inverse Bremsstrahlung, a photon absorbs in an ionic electron system, which raises an electron raises from lower continuum level to the higher one.

Essentially, incoming photon energy converts into kinetic energy. Simple and inverse Bremsstrahlung are very important for laser-generated plasma.

LIBS is relatively new as it was structured first practically applied laser in 1960 [13-17]. Useful data of laser plasma was available before 1977 to determine the mechanism leading to breakdown, measurement of threshold, spark-ignition power density, measurements of power-density and spark ignition threshold, and different parameters pertaining to breakdown threshold intensity.

During the three previous decades, laser-spark spectroscopic literature discussing its development & application is available, which is useful in different fields. This field has undergone magnanimous development since publication of the first report on laser-induced air breakdown in 1963 as researchers made glorious contributions to understand the phenomenon. Various other influences including pulse-width, spot-size, and wavelength were extensively studied.

Pressure-dependent breakdown threshold was first investigated by Mink who studied nitrogen, hydrogen, and helium for pressure range 0.3-100atm through ruby-laser at 25ns pulse rate. Obviously, breakdown threshold intensity reduces when pressure increases by inverse two-third for gases but gas pressure-dependency was different as compared to diatomic gases.

The threshold intensity is dependent on spot sizes and pulse lengths as claimed by Brueck et al [18], who discovered that the breakdown threshold-intensity increases when pulse width increases and decreases when spot sizes increase. Chylek et al[19] investigated the presence of water drops in the breakdown threshold and found that it depends on gas pressure around those droplets. Experts repeatedly conducted experiments with multiple laser wavelengths, which showed that the breakdown threshold intensity is maximum at 0.3-1nm while wavelength threshold intensity of rare gases is 1.06, 0.69, 0.53 and 0.35nm, as mentioned by Buscher et al[20]. Buscher discovered the fact that first threshold intensity rises and later lowers when wavelength increases. Making a comparison between the results of several studies is impossible as they had quite different situations; however, it is possible to give some comments.

LIBS was initially used for atomic detection and molecular identification analyses in 1980s. Moreover, at that time, a few instruments were conceptualized and made using LIBS. This kind of experiments were conducted at Los Alamos National Laboratory (LANL), where Loree and Radziemski did a major improvement in the technique introducing time resolutions [18].

This technology has a main benefit and that is its remote capability, which leads to better detection. An experiment shows that beryllium was detected in the air at a limit 0.5ng/g, and that was 1/3 of the OSHA limit. Later long spark technique (LST) was introduced to conduct spectroscopic analysis of beryllium filtered samples through laser-spark.

LIBS was used to measure trace concentrations of polyatomic molecules in helium as an alternative detection process. The minimum pH levels detectable by monitoring of atomic boron were 434.5 and 336.0nm, which were reproducibly detected B₂H₆ concentration as low as 1 ppm.

An analytical study on laser spark spectroscopy was conducted by Sandia National Labs, and now they are working on monitoring instrument for continuous metal emissions. After gaining the sponsorship of Energy Department of the Sandia Research Group, they are developing a continuous treatment unit.

The group practically showed by measuring 11 toxic metal in the laboratory having concentrations less than 250ppb. Toxic metals such as **B_e** and **C_r** are now measurable at low concentration of **1ppb**. Many studies were conducted to measure spark temperature. The excitation, atom-ionization and electrical discharge plasmas theories are discussed by Margoshes [21].

Spatially-resolved radial excitation temperature as well as radial electron-density distributions were experienced at 15timmm with the help of a torridly shaped and inductively-coupled argon plasma load coil, which was discussed by Kalnicky et al. [21]. Adding excessive ionized elements affected excitation temperature distributions on the aerosol carrier.

The laser-induced plasma and its electron-temperature and density profile in air, argon, nitrogen and helium were tested at 0.5-760torr pressure range. When Grant et al used 11 Fe(I) lines for Boltzmann plot determination, its maximum temperature was observed at 22000K having 760torr air with 0.6mm height to 9000 K for all gases at 0.5 torr with 6.6 mm height from a given surface.

Normally, temperature reduces when the distance decreases from a surface, which reduces ambient pressure. Experiments having flowing liquid samples show that liquid

velocity of maximum 90cm/sec has no effect on analytical outcomes. The sizes, velocities, and elemental compositions of particles during combustion flow are also assessed through laser spark spectroscopy.

Sandia National Labs developed laser-spark spectroscopy. Identification of 3 bituminous coal samples with varying geological origins were brought, and different quantities of coal types was conducted.

It was found that coals had different amounts of elements such as Li, Na, K, Mg, Ca, Ba, Sr, and Ni, Ti, Si, K, Mn, Fe, C,H,O and N, which were observed in the spark spectra. Schmieder and Kerestin[22] demonstrated laser spark diagnostics for monitoring combustion-product elements with the help of N₂ and O₂. The abundance of n atoms has been measured using spark emissions. During a later experiment, fuel-to-air ratio was determined in a methane lamp through finding C/N ratio.

Spatial data was collected with the help of moving spark inside a flame. Relative abundance of H, C, N, O and shale oil vapours were determined as a part of our work for the current study. Researchers including Radziemski et al found laser electron-density as well as temperatures that produces air plasma.

The electron-density ranges from 10¹⁶cm⁻³m. Time-resolved LIBS of aerosol was observed by Radziemski et al., who predicted that immediately after plasma initiation, two materials decayed leaving neutral emission lines between 0.1 and 1. During intermediate and later times, (>5ns) molecules retained their features. They observed quiescent time-period between 1 and 20us after reducing background emission and keeping the neutral line intense. They believed that the stark-broadening is important for spectral line width for many LIB plasma species specifically during earlier detectable situation of neutral perturbs in LIB plasma, which is more than the charged particle density by factor 10. In the LIB, plasma occurs after 10us.

Doppler width plays an important role in many cases. Doppler width N415 nm at us is 0.01nm, whereas the stark width remains 0.76nm. Other extreme for Be II 313nm mainly contributes towards line width. Many lines that we observed had widths between 0.1 and 0.3nm. Kyuesok et al. observed line broadening for copper plasma through THRLIBS by experimenting in Helium-rich environment. Xianglei et al predicted that the intensity of double-pulsed LIBS is initially twice as much when the

delay-time changes from 100 to 200ns, which is also true for laser pulses, temperature and electron number density, which abruptly change within the same timeframe. Barthelme et al. observed space-and-time-resolved measurements of electron density and temperature of laser- and reported that dependence of plasma properties on pulse duration.

While analyzing plasma properties, they opined that the plasma expansion has agreement with the Sedov's model [23] in the initial 500ns, and then, it gets subsonic as far as velocity of sound after plasma creation is concerned.

CHAPTER 3

Atomic Emission Spectroscopy

3.1 Introduction

Light emissions from gaseous substances were examined by using spectrometer from spectrum, which consists of discrete lines/bands/overlying continuum [24]. They have three fundamental features:

1. Wavelength
2. Intensity
3. Line shape

These properties depend on the environment of emitting atoms and their structures. Atomic emission spectroscopy is helpful for finding the identity of a structure and/or temperature of atoms through analyzing their radiation. By measuring wavelength, we may find out atomic energy levels and provide experimental foundations to support/criticize atomic structure theories. Measuring intensity of each spectral line from a provided source gives the line intensity information. Physical parameters of discharging sources like temperature and pressure have an impact on the intensity and spectral line shape.

3.2 Radiations from Atoms

The spectral line intensity is based on:

1. Basic level excited atomic population
2. Final intrinsic transition probability as defined by Einstein's A & B coefficients exhibited in the diagram below:

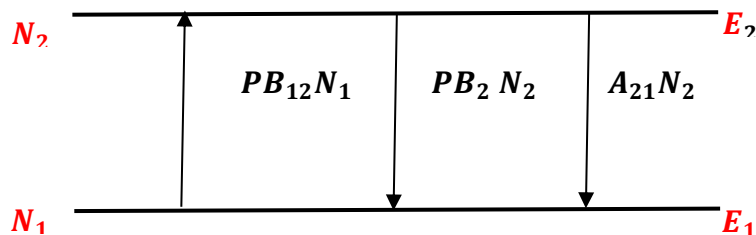


Figure 3.1 Emission and absorption process between two energy levels.

Where E_1 & E_2 are discrete atomic quantum levels having N_1 and N_2 atoms/cm³ populations.

The spectral line frequency between two levels is:

$$h\nu_{12} = E_2 - E_1 \quad (3.1)$$

3.3 Electric Dipole Transition Selection Rules

When we suppose that the external electromagnetic radiation is time-dependent, it can be effective for stimulated emissions $E_2 \rightarrow E_1$. For absorbing $E_2 \rightarrow E_1$ to make both states non-degenerated.

For absorption $E_2 \leftarrow E_1$ so that $B_{21} = B_{12}$ when both states are non-degenerated.

Here, B coefficients is calculated through quantum mechanics through treatment of oscillating and magnetic fields in a time dependent perturbation, which leads to the following expressions

$$B_{12} = (2^2 / 3 \epsilon_0 h^2) [M_x^2 + M_y^2 + M_z^2] \quad (3.2)$$

Here ϵ_0 represents free space permittivity M_x , M_y and M_z are parts of the transition moment vector M_{12} that is as follows:

$$M_{12} = \int \psi_{j_2}^* \mathbf{r} \psi_{j_1} d\vec{l} \quad (3.3)$$

Where ψ_{j_2} and ψ_{j_1} are the wave functions for upper & lower states respectively.

Here " \mathbf{r} " is operator, which corresponds to electronic displacement of the atomic charge.

Here " \mathbf{er} " denotes dipole moment-vector. The defining quantum numbers explain that wave functions approve some relations for non-zero transition moments called as selection rules, which apply to the total angular momentum quantum number "j." It is given by:

$$\Delta J = J_2 - J_1 = 0, \pm 1 \quad (3.4)$$

3.4 Forbidden Transitions

Some transitions, are forbidden during dipole approximation, which appears to be as weak as quadruple/magnetic dipole-radiations.

The electric quadruple radiation matrix elements are

$$Q_{12} = \int \varphi_{j_2}^* \hat{Q} \varphi_{j_1} d\tau \quad (3.5)$$

They do not finish when they possess same parity because the operator x y parity is clearly even. φ_{j_2} and φ_{j_1} possess same parity like what operator x y does.

3.5 Oscillator Strength

Classical emission model shows that atomic emission means electrons' showing simple harmonic motion at characteristic frequency ν while the amplitude reduces subsequently.

Since energy radiates, radiation emission performs like a damping agent for the motion of the electron motion. Since m is electron-mass and $\tau = (2\pi e^2 \nu^2) / (3\epsilon_0 m c^3)$ order 10^{-8} sec for visible emission.

Here m represents electron mass and $\tau = 1/\gamma$ of order 10^{-8} sec for visible emission. As light travels within an absorber medium, atoms absorb energy, which is proportional to that medium's thickness.

Incident flux of light L thickness of the medium

$$I(L) = I(0) \exp(-K_\nu L) \quad (3.6)$$

Where ν means frequency across thickness L and $K_\nu \text{ cm}^{-1}$ called as absorption coefficient.

3.6 Intensities of spectral lines

The spectral line's observed intensity relies on two things:

First factor is transition probability/ line strength/f-value. Second factor depends on excited states when an emitting medium spontaneously produces a photon. Now low

pressure gas discharge takes place and an electron's kinetic energy is distributed. Here electron temperature is valid as a concept.

The atomic electron-impact excitation probability is generally high. Equilibrium is a discharge source when the energy exchange takes place more rapidly between atoms and electrons in comparison with the excitation rate. When two spectral lines emerge out of maximum energy levels I_1 and I_2 , transition probabilities A_1 , A_2 and line strengths S_1 , S_2 can be expressed as follows:

$$\frac{I_1}{I_2} = \frac{A_1 N_1}{A_2 N_2} = \left(\frac{A_1 g_1}{A_2 g_2} \right) \exp(E_2 - E_1)kT = (S_1 V_1^3 / S_2 V_2^3) \exp(E_2 - E_1)kT \quad (3.7)$$

Where $k \rightarrow$ Boltzmann constant \rightarrow gas Temperature in Kelvin.

Spectral lines with lowest excited atomic levels in upper, ground, and lower atomic states are called as rejoin (resonance) lines.

These lines emit light as they have maximum re-absorption probability earlier than plasma discharge, and this process is called as self-absorption.

A level becomes "met stable" when all transitions towards low level occurs having small probabilities because of the selection rule.

3.7 Continuous Emission and Bremsstrahlung

$$H_\nu = \epsilon - E_j + \frac{1}{2}mv^2 \quad (3.8)$$

Where $\frac{1}{2}mv^2$ is kinetic energy and ϵ is ionization energy of the atom.

The transitions exist between Free State $\epsilon \rightarrow$ ionization of atomic energy and stationary atomic state E_j , which gives rise to continuum emission.

Emission process is called radioactive recombination. Free-free emissions correspond with the kinetic energy losses through an electron in an ionic field.

The emission results in deceleration and is termed Bremsstrahlung, which means braking radiation in German.

3.8 Broadening of Spectral Lines

Spectral line intensity is dependent on the atom that emits radiation Lorentzian profile with the following form:

$$I(\nu) = \frac{I_0 \left(\frac{\gamma}{4\pi}\right)^2}{[(\nu - \nu_0)^2 + (\gamma/4\pi)^2]} \quad (3.9)$$

Here, I_0 central intensity the profile ν_0 and γ is the radiation.

The intensity spread over different frequencies is termed as natural spectral-line broadening. And $\gamma/2\pi$ is termed as full-width-at-half-maximum (FWHM). Doppler broadening dominates shape of the line near its centre.

Doppler broadening takes place as a result of random atomic thermal motion, so the resulting profile is Gaussian having FWHM given by:

$$\Delta\nu_0 = (2\nu_0/C) (RT \log 2/M)^{\frac{1}{2}} = 7.16 \times 10^{-7} \nu_0 \left(\frac{T}{M}\right)^{\frac{1}{3}} \quad (3.10)$$

Where ν_0 the velocity of line centre, M represents atomic mass while T shows equilibrium temperature.

Dense plasma surrounds itself with radiating atoms, with above broadening mechanisms, which lose their significance when broadened by charged particles. It is given that the atom has interaction with charged particles by means of electric field, which is termed as Stark broadening. Two important reasons determine line shapes of plasma.

The first reason is line-shape usage for determining emitting plasma's physical properties including particle density and temperature.

The second is determining both induced emission as well as absorption coefficients, which rely on oscillator densities of emitting atoms.

Determination of Electron: when molecular vapour temperature increases, molecules dissociate into atomic form and further transform into ions plus electrons.

These molecular atoms and ions should be excited for providing them with high energy state and raising their kinetic energy.

The spectroscopic radiation analysis depends on local equilibrium conditions.

3.9 Temperature and Equilibrium

Maxwell's distribution for particle velocities having mass (M) shows that the particles are moving within velocity range v to $v + dv$. Their number density N and temperature T will be:

$$d_N(v) = N \left(\frac{M}{2\pi KT} \right)^{\frac{3}{2}} \exp \left(-mv^2 \frac{1}{2KT} \right) 4\pi V^2 dV \quad (3.11).$$

The Boltzmann distribution for particles N_j with excitation energy E_j will be:

$$N_j = N \left[\frac{g_j}{u(T)} \right] \exp (-E_j/kT) \quad (3.12)$$

When $u(T) = \sum g_j \exp(-E_j/kT)$, it is termed as state sum/partition function.

The equilibrium condition can be obtained through Saha's equation.

$$\frac{(N_e N_i)}{N_o} = \left(\frac{2(2\pi m k T)^{\frac{3}{2}}}{h^3} \right) (U(T)) / (U_o(T)) \exp(-\epsilon/kT). \quad (3.13)$$

N_e represents electron number density while N_i and N_o is electron densities of ions and atoms respectively.

CHAPTER 4

EXPERIMENTAL TECHNIQUE

4.1 Introduction

There are different experimental techniques for spectroscopic investigation of solids. These are mostly based on spectroscopic absorption/emission.

As discussed in the Chapter 2, absorption/emission spectroscopy are the most applied methods for analysing and finding trace contents of solids, liquids or gases. These experimental techniques were improved in precision and sensibility by applying laser light as an excitation tool. An important experimental technique for analysing the contents of materials is LIBS.

4.2 Laser-induced Breakdown Spectroscopy

As mentioned earlier, LIBS determines any sample's chemical/elemental quantity using laser ablation through emission of atoms, ions, and molecules. Figure 4.1 shows the schematic diagram for LIBS experimental setup.

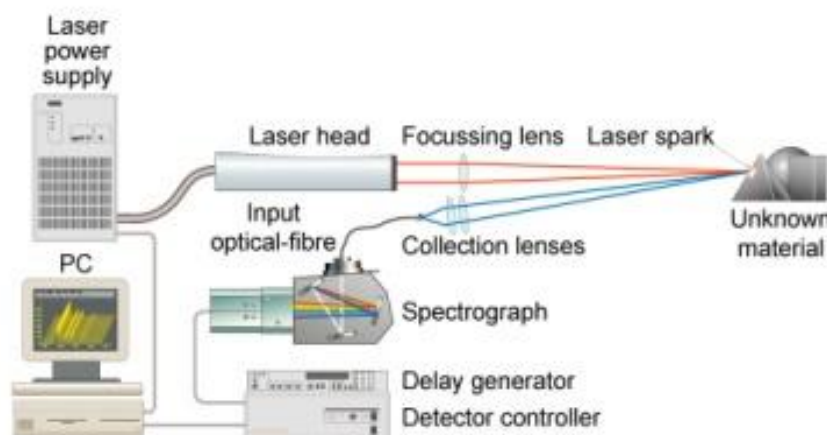


Figure 4. 1 Overview of Experimental Set Up for LIBS

In LIBS, plasma generation is done using high-intensity laser on a target surface whereas the atomic emission signal from the plasma is detected for solid substance analysis [10]. Since laser's power density has to be greater than the threshold value for generating laser-induced plasma, laser beams utilized for LIBS processes are normally high-powered and have narrow signal output. LIBS uses laser for material analysis and determining gas composition. High energy laser focuses sharply on a point generally at 40mJ/pulse for 10ns pulse width that corresponds with 10 GW/cm² focused power density, which is enough to generate plasma.

High temperature plasma with more electron-density is used for spectroscopic radiation analyses for radiation that emits out of plasma. For determining composition, properties and some aspects of the analyzed sample, the mentioned method is used, which is termed by several notations. Other than LIBS, TRELIBS (Time Resolved Laser-Induced Breakdown Spectroscopy) and LSS (Laser Spark Spectroscopy) are other terms, which describe the same method.

LIBS and TRELIBS have many common benefits including non-invasiveness, no electrodes to disturb plasma and real time detection. Moreover, TRELIBS offers temporal resolution; therefore, it lowers detection limits. LIBS has several benefits such as inductively coupled plasma (ICP), atomic absorption spectroscopy (AAS), atomic emission spectroscopy (AES), and atomic fluorescence spectroscopy (AFS), which are commonly utilized for determining abundance of elements.

Moreover, they provide reasonable detection limits, sensitive and selective operation facility, multi-element function and reasonable cost. Atoms can be passed through excitation process when their temperature is raised by applying a flame, inductively-coupled plasma, or spark. The absorption signal is generally found out by finding reduction of transmitted "negative" signal.

Sometimes, there is zero emission signal and at that point we calculate emission-measurement with sensitivity and later find out the total absorption. LIBS has all sorts of emission source issues, and spectral line interferences. Still, it has many significant advantages as well. They are given below:

Whenever source brightness is too much, the spatial/temporal resolutions may be more as well, and besides, the atomic specs become accessible given that the energy is enough. They are free of molecular composition.

The molecular bonds are easily breakable, so, no sample preparation is needed, and besides, little sample quantity is sufficient for applying this procedure. No physical interaction with samples is needed and a sample's physical state does not matter. The plasma is generated in a simple way as laser pulses vaporize and excite the sample's atoms without auxiliary analysis, which makes the process cost-effective.

Since it is an emission process, it offers multi-element analyses simultaneously. It is possible to generate the spark in remote places, it is helpful for non-invasive analyses because it needs just optical access.

4.3 Some Applications of LIBS

LIBS normally needs very less sample preparation, so it is easy to use it in the field and it is suitable for dangerous industrial zones. Practically, LIBS is used soil and mineral analyses exposing mineral qualities (for mining, geology and, civil engineering). Express analysis of other planets is continued for analyzing conditions on other planet such as Venus and Mars, environmental conditions (quality of water and air, industrial sewage and other emissions), and biological content (hair and teeth, bacterial species, bio-aerosols, anthrax, airborne infections, virus, allergy-causes, fungal moulds and pollen). They are used in so many areas, which are beyond the scope of the current work.

4.4 Overview of the Experimental LIBS

LIBS is a atomic emission spectroscopic process, which uses intense laser pulses to produce plasma from samples. Plasma light emission can give “spectral signatures.” LIBS analysis is generally accurate economical, and speedy but it has certain detection limitations; however, it is a very popular atomic analysis technique

4.4.1 Principles of the Experimental Method

When intense laser pulse focuses, di-electric breakdown takes place, which leads to plasma formation releasing different atoms and molecules in the environment.

When plasma is cooled down, atoms, which are in excited state, release light energy with certain wavelength range between 200nm to 900nm. These emissions are resolved and noted only 1 microsecond after the pulse, which shows elements present in any sample. The application of high-intensity laser creates “plasma spark”. This process excites and ionizes atoms by giving them specific energy levels. The atoms and ions later decay leaving “fingerprint” elemental emission line spectra [2].

4.4.2 Laser as Light Source

In LIBS experiments, Nd: YAG laser is a powerful light source to create the plasma of the sample. Use of Nd: YAG laser is new for conventional processes including XRF (X-ray Fluorescence) or ICP (Inductively Coupled Plasma). It saves time and besides, it is an economical option for testing elemental concentrations. Nd: YAG absorption takes place at 730–760nm & 790–820nm.

At low-current densities, krypton flash lamps are good light sources at approximately 900nm. Nd: YAG exists in crystalline form. Do pant, triply-ionized neodymium, and Nd (III) replace some yttrium ions within the host crystalline structure.

Neodymium ions make leasing activity possible within a crystal exactly what red chromium ions do for ruby lasers. Crystal YAG host is given about 1% neodymium. Nd:YAG lasers/their variants need flashtubes, gas-discharge lamps, or quasi-infrared laser-diodes for the pumping process.

Pre-stabilized laser (PSL) is a type of Nd: YAGcategory, which provides strong laser to gravitational wave interferometers including VIRGO, LIGO, GEO-600 and TAMA [6]. The lasers emit parallel beams, which are collected using lens then the excited sample emits characteristic radiation, which is again collected by fibre and radiation is transferred to spectrograph and detector.

4.4.3 Excitation by Laser Light

For exciting and reaching an excited energy level, some energy must be provided to the atom. After having excited an atom to an allowed energy situation, it tries to move back to low-energy states mostly to the ground state. The optical transitions to lower states within the atom lead to photon emission having energy according to the energy differences between the transition levels, when the transition occurs. For two energy-

levels, $\Delta E = h\nu_0$, the emission rates of photons of energy E at a frequency ν_0 are obtained.

So, the emitted photon has the frequency, which is appropriate for absorbed frequency, and the laser frequency applied in absorption process should be in a broad distribution, so during the excitation, all the desired levels would be occupied. As LIBS light source, selective excitation is required to increase the excitation.

Although many lasers have necessary features, high energy Nd: YAG laser pulses with 1.06 μm fundamental transition wavelength and the 2nd harmonics ($\lambda = 532 \text{ nm}$) are mostly considered as light sources. (Nd-YAG) in our experiment used wavelength in the green laser 532nm and also 1064 nm, which are second and first harmonics respectively. The arranged wavelength on spectrometer is between 200-1000nm while laser pulses have 25mJ.

4.4.4 The Fibre Optical Cable

Optical fibre cables are transparent and flexible fibres manufactured using glass and plastic. They are thick probably negligibly thicker than human hair. It transmits electromagnetic signals to the apparatus detector. It consists of a bundle of glass threads.

Optical fibers generally have transparent core coated with transparent cladding materials to minimize refraction. Light signals move through the core and data is transferred through them. Some optical fibre cables are multi-mode while others are single mode but they have capacity to transmit large quantities of data at the speed of light.

Multi-mode fibre consists of wider core, and they are useful for short distances and high-power transmission. Single-mode fibre helps when communication lines are more than 1,050 meters [25]. Temperatures of laser-induced plasma and electron density are measurable. The element "t" has less concentration, which works on higher resolutions.

4.4.5 Advantages

Echelle system has a comparison with Czerny Turner spectrometer at 1-m focal length and 3600 lines/mm grating. It helps avoiding spectral interference. Another significant factor is its broad coverage range 200 to 780nm. It helps analyzing complex matrices. Echelle's spectrometer is a valuable device because it almost instantaneously recognizes elements of an unknown sample.

Echelle spectrometer helps changing resolution at wavelength more than 600nm despite the fact that the CCD detector receives just a few electrons. After increasing the gate-width, intense emission lines can saturate some CCD pixels. Moreover it has low data acquisition rate. CCD resolution is only 1024× 1024 pixels while PC board works on 500 KHZ at 16-bit resolution.

4.4.6 The Detectors

We take broadband array spectrometers, simple CCD (Charge Coupled Device) based spectrometers, and Echelle spectrometers having intense CCDs..

They also have intense PMT (Photo-Multiplier Tube-based) spectrometers. Their special characteristics and features are described as follows:

CCD-Based Spectrometers are useful, inexpensive and offer more coverage [26].

A charge-coupled CCDs are micro devices, which process memory signals perform imaging). CCDs have electronic analogue with magnetic bubble. For acting as a memory, they need some physical quantity for to represent some information. CCDs' four major tasks include generating, collecting, transferring and detecting charge.

4.4.7 Broadband Diode Array Spectrometers

They are CCD-based detectors for broader wavelength ranges. Typically uncoupled, multiple-CCD spectra are joined together for making broadband spectrum 563, and these systems are economical and multi-element sensitive. Diode array spectrometer can be made with either reflection or transmission diffraction for any given spectrometer configuration (mirrors/ Lenses, grating, and detection).

Their wavelength range and resolution can be changed by exchanging the diffraction groove density. For spectrometers based on reflection gratings, it is possible to manage the wavelength range by rotating the grating. This is however not possible with spectrometers based on transmission gratings.

4.4.8 Echelle Spectrometers

They have intense broadband with higher CCD, which allows spectral acquisition of upto 10 nanoseconds grating. Echelles disperse light through prism and gratings on the detector, which results in 2-dimensional spectral-field. [27].

4.4.9 Czerny-Turner Spectrometers

This disperses light with the help of grating, which is normally first order of grating. On 256x1064 high intensity CCD, very high light dispersion is experienced. That intense first-order light along with binning from 1-256 rows camera intensifier of 1-256 results in incredible range [28].

4.5 Photomultiplier Tube (PMT)-Based Spectrometers

A photomultiplier is a point-detecting device having high potential gain as compared to intensified CCDs because of many gaining stages. They can give 10⁷ signal amplification to a CCD's 5 x 10⁴, which is higher as compared to two magnitude orders. But they are utilized as point detectors in broad arrays or multiple detectors as a part of Paschen-Runge spectrometers.

4.5.1 High-spatial resolution

It is needed for 2D solid substance profiles having upto 1 μ m accuracy. So little or no sample preparation need exists in addition to less time for measurement, more convenience, and low contamination chances. Samples may exist in any physical form. The process of analysis is accomplished even with trace sample quantities exist in nanograms, which is helpful in chemistry for new chemical research and in material sciences for analyzing composite materials or nanostructures.

Virtual analysis of every chemical/element is possible even when sufficient quantities of those elements in unavailable. It is even possible to analyze very hard/brittle

materials like ceramics and superconductors. In aerosols, both sizes of particles and chemical composition are simultaneously analyzed [3].

4.6 Pharmaceutical Applications

Blend Uniformity

Uniform API blend and chemical (lubricants, disintegrates, compaction agents) are directly related to product performance. Blend uniformity can be impacted by many factors like particle sizes and shapes, surface characteristics, electrostatic interactions, moisture content, environmental humidity and blender configuration. LIBS is helpful for monitoring homogeneity of a species (API, lubricant, etc.) within a tablet, within a batch, and between different batches. LIBS signal %RSD is the most useful indicator of blend homogeneity[4].

Film Coating

Film coating is used to quote tablets. It protects against air, moisture, and light, and they cover up bad taste and improve ease of swallowing. Improved photo-stability often depends on thickness of film and amount of pigment. LIBS is helpful for monitoring coating composition, thickness and uniformity with little-to-no sample preparation. The depth-profiling capabilities of LIBS are useful for layer-analysis Quantification of various pharmaceutical components, phosphorous containing active APIs in microcrystalline cellulose and hydrous lactose matrix were analyzed at w/w concentration ranges of 0-5% active agent (0 to 0.95%p). Mg has many atomic and ionic lines chosen for measurement, in this case, calibration curves were constructed for Mg 518nm and Mg 285.21nm [5].

4.7 Investigation and classification of pharmaceutical tablets

LIBS technique is able to find out and analyze organic as well inorganic tablet constituents in a one-step procedure, which is a great convenience. This is not possible with any other process including ICP-OES and ICP-MS. Finding organic constituents can be very useful during the drug discovery stage and during drug production as well.

Additionally, LIBS has a potential use for collecting drug/chemical formulation, which helps during the process of drug screening. In LIBS, several peaks are attained within

200 to 1000nm spectral range [29]. Wavelength of emissions is atomic/ionic property, which exists within the obtained plasma.

Solid samples are treated in a genuine situation for experimentation [30, 31]. Total time required to conduct experiments and achieve results is too low. High-power laser and sensitive detectors enabled expert to conduct LIBS procedures from a distance of a few meters, which makes it appropriate for on-site and remote usage in many industrial processes.

4.7.1 Detection of Elements Distribution in Drugs

Pharmaceutical tablets are quantitatively and qualitatively analyzed utilizing LIBS. This technology has many benefits such as speedy and accurate analysis without much need for sample-preparation.

Using LIBS, elements distribution in drug tablets can be fast and easy. This method could be set up to determine distribution as an innovative tool to help methodical development and test the tablets blend uniformity [6].

4.7.2 Classification

For analysing and classifying different pharmaceutical tablets, many methods such as Cluster analysis (CA), Neural Networks (ANNs), Principle Component Analysis (PCA), and SIMCA may be utilized.

4.7.3 Cluster Analysis (CA)

Cluster analysis/clustering assigns objects in clusters keeping in view that the objects in a cluster are similar to each other [32].

4.7.4 Clustering algorithms

Connectivity-based cluster or hierarchical clusters focuses on objects being highly similar to closer objects as compared to those, which are on a distance. Algorithms convert objects into "clusters" with respect to their distance.

Centred-based clustering: or k-means clusters:

This type of clusters is based on central vector and that vector may not be part of the data set. K-means clusters imply that the numbers of clusters are fixed. In that case, cluster centres are found and their objects are assigned to the nearest cluster centre for minimizing their distance from the cluster.

Distribution-based clustering. This type of clustering relies on distribution models. Clusters are groups of similar objects.

4.8 Principle component analysis (PCA)

It is mathematical process that utilizes orthogonal transformation for converting possibly correlated variables into linearly uncorrelated variables or principal components [7]

4.9 Artificial Neural Networks (ANNs)

It is a mathematical model, which gained inspiration from neural networks, and it is a biological concept. Every neural network contains artificial neurons, which process information with the help of "connectionist" computation approach (Fig. 4.2).

A neural network undergoes structural changes during the initial learning phases but still it helps finding complex relationships between outputs and inputs, and it also helps finding patterns, which are quite helpful.

Artificial neural networks work with the help of strong connections to generate a desired signal flow, which is very much like biological neuron flow. The "neural network" concept is borrowed from psychology and it is applicable in some other sciences as well. Neural models are very important theoretical/computational neuroscience concepts. Historically, these models forced conceptual change in 1980s from symbolic artificial intelligence (AI) to sub-symbolic intelligence.

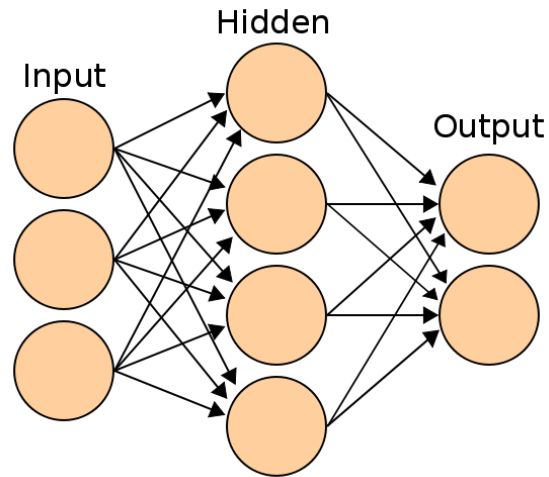


Figure 4. 2 Artificial Neural Networks

The idea of neural networks was taken from the structure of human CNS (central nervous system), which is artificial having nodes, called "neurons", "neuroses", "processing elements" or "units" because they link with each other forming a whole network just like biological CNS.

No single agreed upon definition of artificial neural network is available. It is simple processing network, which shows complicated behaviour through connections between elemental parameters. Artificial networks work with the help of algorithms created for altering the connection strength for creating the needed signal flow.

They have stark similarities with biological networks, which jointly perform in parallel without any clear delineation. The terminology "neural network" means those models of statistics, cognitive psychology and AI, which emulate human nervous system.

Sophisticated artificial neural networks are biologically inspired but some of them were abandoned because practical models based on statistics and signal processing perform better. Some of their components including artificial neurons combine adaptive as well as non-adaptive elements. These adaptive systems are appropriate for real-life problem-solving, but they have little to do with traditional artificial intelligence models. In the past, neural network models created paradigm shift in 1980s with the symbolic concept of artificial intelligence [8]

4.10 SIMCA

SIMCA (Soft independent modelling by class analogy) is statistical process for specialized data classification, which requires training data sets, specified attributes and class groups. Here "soft" indicates that the classification involves multiple classes.

Firstly, the samples in every class should be assessed with the help of PCA on significant components also considered as principle components. There is a need for maintaining critical distance using F-distribution generally calculated at 95% or 99% confidence levels. The observations are processed with the help of the PC model and residual distances are found out. Every observation becomes part of a model class and the calculated residual distance remains lower than the statistical limits for that class. The observation might fall in many classes and it is quite possible to find measure of goodness from many cases while the observations are placed in multiple classes. Classification efficiency can be indicated through receiver operating characteristics.

4.11. LIBS instrumentation

LIBS process was recorded with the help of "Quintal-Big Sky" Nd:YAG laser (Bozeman, MT, USA) Ocean optics Spectrograph (Dunedin, FL, USA) and Stanford's Delay Generator SRS DG535 (Cleveland, OH, USA). Figure (3) shows the LIBS setup.

The laser works at 532nm wavelength, which applies for ablation of samples. It later ran in Q-switched mode at 1Hz with 0.5ls gate delay and 20ls gate width. Samples were processed using LIBS through scans of five locations and 4 excitations.

LIBS is very helpful to analyze tablet coating in pharmaceutical industry because it helps calculating coating thickness. Coating thickness is correlated with tablet weight, which cross checks and validates LIBS analysis. The laser-shot frequency has no significant effect.

4.12 Experimental Procedure and Recording Emission Spectra

The plasma emission spectra help us study the temporal electron density's evolution in plasma while expansion and perishing. Electron density was found through Hydrogen Ballmer line's (Ha's) stark broadening at 656nm, which is good to determine electron

densities because that is isolated and intense because of substantial hydrogen concentration in organic substances. Moreover, linear Stark effect influences this line because of degeneracy of the lower level [26].

CHAPTER 5

EXPERIMENTAL METHODS AND DATA ANALYZES

Electron density determination is mentioned for laser ablation plasma diagnostics[41]. The electron density is as under [26]:

$$N_e(H_\alpha) = 8.02 \times 10^{12} \left(\frac{\Delta\lambda_s}{\alpha_{1/2}(N_e, T)} \right)^{3/2} \text{ cm}^{-3} \quad (7.1)$$

Here $\frac{\gamma_1}{2}$ is half width of angstrom stark profile. Its parameter $\alpha_{1/2}$ partially relies on excitation temperature and electron density. Parameter values are given [26] with 10% precision. For extracting stark line width, LIBS spectra are adjusted by means of Voigt profiles.

An example associated fitting curves and spectra by means of Voigt profiles have been exhibited in Fig. 3 with detection delays 100 to 1000 ns.

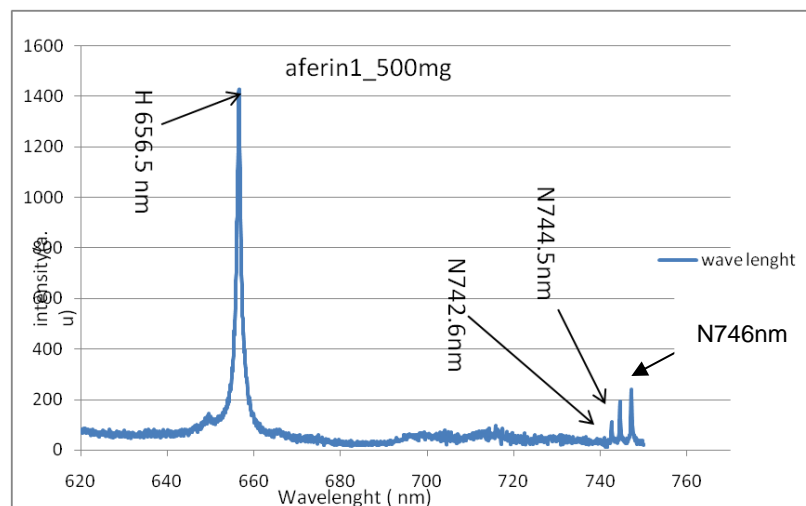


Figure 7.1 The properties of intensity and wavelength of aferin tablets show hydrogen 656 and nitrogen 742. 744

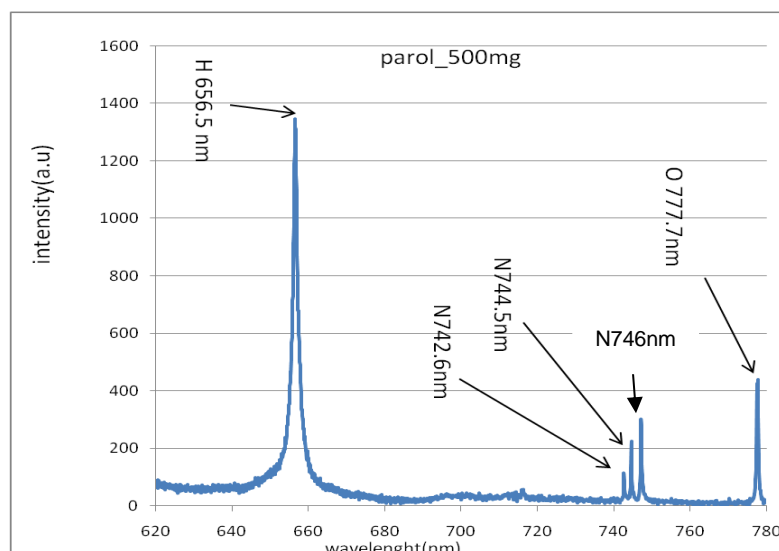


Figure 7.2 The properties of intensity and wavelength of aferin tablets show hydrogen 656 and nitrogen 742. 744 and oxygen 777

The over-the-counter drugs were bought at a pharmaceutical store/drugstore. They were scanned using LIBS for any further processing. Table 1 shows the details about it. The spectra initially records coating in the coated samples.

(The tablets were color-coated samples.) The rules and laws mentioned in [42] apply for coating removal that assures sample flatness.

Table 7.1 Details of pharmaceutical samples

Se. No.	Sample name	Primary Formula	Ingredients
1	Parafon 300 mg	$C_8H_9NO_2 + C_7H_4ClNO_2$	Paracetamol+ Chlorzoxazone
2	Parol 500 mg	$C_8H_9NO_2$	Paracetamol
3	Aferine 650 mg	$C_8H_9NO_2 +$	Paracetamol+ chlorpheniramine maleate

Five to ten different pharmaceutical tablets were purchased from a local drug store. They will be scanned using LIBS for further processing.

The experimental setup Figure (7.3) shows the LIBS setup. The laser works with 532nm wavelength and utilized for sample ablation. Later, it was processed with Q-switched mode at 1 Hz repetition rate.

We performed external gated detection with 0.5ns gate delay & 20 ns gate width. Spectrograph was operated to emit laser in the form of pulses with the delay generator. Samples were processed using LIBS for scanning five parts and four excitations.

The variability was insignificant and the analysis showed inadequate mixing performance of tablet coating device.

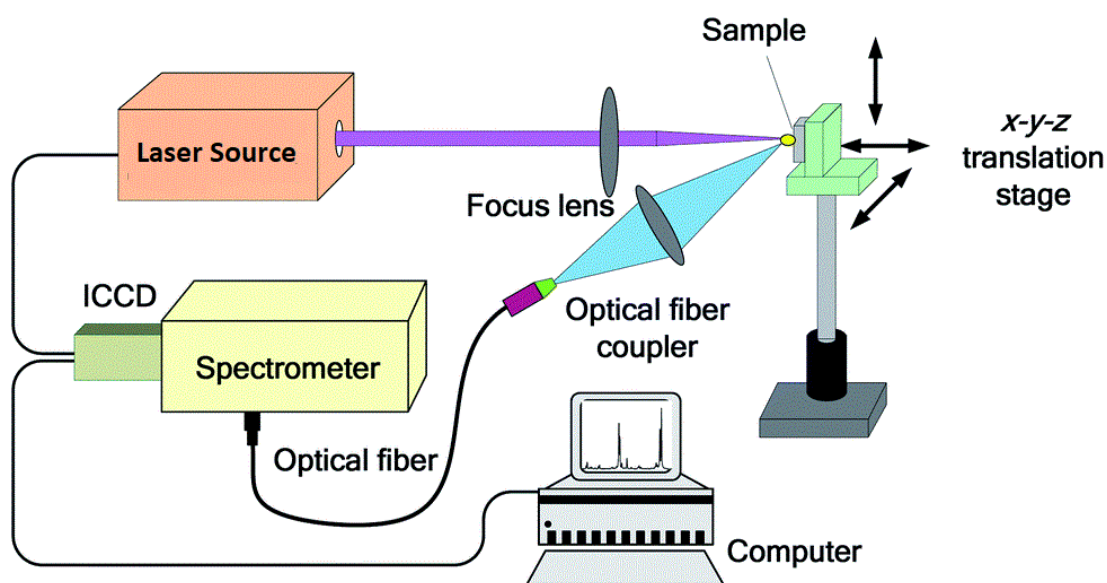


Figure 7.3 Experimental set up

5.1 Introduction

Principal Component Analysis (PCA) is in fact variability analysis tool for a particular set of data. Experts also call PCA a "workhorse" of a variable method. PCA is a highly facilitating method because it offers a set of graphic tools, which help researchers understand link between variables and samples. PCA has been recognized as a universal data mining tool, which any person can use for different situations. It is more effective for voluminous data with 10 or more variables or as many as 100 samples. In some applications, PCA points out failures in a process, for example, market analysis, business intelligence and drug discovery.

Drug discovery: Drug molecules are investigated especially when new drugs are introduced either over-the-counter medicines or patient-specific ones.

Pharmaceutical analysis: It is important to locate raw materials either through PCA or by NIR (Near Infrared) spectroscopy.

PCA is useful both on industrial and research levels because sometimes, it is used to detect onset process failures. It also helps understanding properties of new drugs.

PCs help describing sets of data. The evaluation depends on how appropriately a sample is modelled. Every PC gives information. The first one describes greatest variability. When all PCs are combined, they give information through few PCs and the remaining is considered as noise.

The PCA can be expressed through following equation:

$$\text{DATA} = \text{INFORMATION} + \text{NOISE} \quad (5.1)$$

Here noise means whatever was leftover.

Scores plot: It creates a map showing variables.

Loadings plot: In addition to scores plot, loadings plot also has a map.

5.2 Some General PCA Guidelines

While assessment of the PCA, experts should consider these guidelines: Give priority to the variance plot and make a calculation as to how many PCs are actually needed for describing variability. The fewer the PCs are, the better the outcomes will be. A researcher should observe PC1 versus PC2 and find possible patterns, which show small and easily manageable data structure concerning important phenomena. Use of loading helps knowing highly contributing sample groupings, which gives more clarity. Using influence plot helps understanding if the samples are well-represented by the model for determining the presence of any extreme sample.

5.3 PCA and Classification

The common method using PCAs is SIMCA. For using PCAs for classifying initial event detection, some limits should be defined.

The classification is separation of groups for distinctive features in the objects. Here, we have a couple of approaches to classification: unsupervised and supervised. Supervised classification: It is utilized for multivariate classification problems and is used during SIMCA or PCA.

It uses the following methods:

- Linear Discriminate Analysis (LDA)
- Logistic regression
- Partial Least Squares Discriminate Analysis (PLS-DA)
- Support Vector Machine Classification (SVMC).
- Unsupervised classification: It uses the following methods:
 - K-means
 - K-medians
 - Hierarchical Cluster Analysis
 - Principal Component Analysis

5.4 VARIANCE AND GOAL

Here, our most important question: What best expresses the mean of the data?

This section will answer this question and discuss additional implications as well. In the end, we will discuss mathematical objective to decipher “garbled” data, which means redundancy and noise.

Noise: Noise percentage should be low in any data irrespective of the data analysis technique; otherwise, no information about a system can be extracted.

Redundancy: Redundancy is a trickier issue as it makes data irrelevant.

5.5 Principal Component Analysis

The LIBS is a successful process of analyzing corrosive and dangerous chemical/biological samples and it depends on statistical methodologies for quick analysis. [33].

Many statistical processes interpret spectroscopic data including industrial process monitoring, forensic evidence studies and biometrical identification. They are called

as chemo metrics. Scientists and researchers sometimes use them for analyzing hazardous substances and on many occasions, their feasibility was established.

They include linear correlation analysis, PCA and SIMCA, and so far, they have been utilized for analyzing many biological stimulants, biological interferences, and chemical stimulants. Some researcher applied all the three statistical processes.

PCA reduces information with variable combinations or principal components in a set of data. For every PCA, score is obtained regarding individual principal component loading. Principal component score gives information about the sample, and loading described by the correlation between the concerned variables.

PCA data representation tools include scores plot and a graph. PCA is redefined for every sample segment, and the consequent model is used for residual variance pertaining to every category.

The outcomes are further processed through F-test to finally find out most probable category of the samples. Details of SIMCA and PCA are available in the literature. Experts claimed that the given analyzing processes are partly successful for differentiation of single-shot emission spectra using samples. Spectra averages and variance-weighting processes gave the best outcomes/results. The sample identification through LIBS can be challenging as it becomes possible after creating a reliable statistical model and pre-treated data.

There was a need for more investigation to find shot-to-shot variation sources specifically plasma temperature and volume, and matrix effect. As a part of my thesis, I have conducted a software analysis using PCA data and compare experimental work and software assignment.

5.5.1 What is a Principal Component?

Technically, principal components are linear combinations of weighted variables. For understanding them, we should finalize how to compute subject scores as a principal component.

5.5.2 Characteristics of Principal Components

The initial component is taken out of principal component analysis, which has maximum variance among all the tested variables, which implies that our major component is definitely correlating with many or a few variables. This also means that second component is also correlated with a few variables. Moreover, second component's second characteristic must not be correlated with initial/first variable; therefore, correlation between first and second components must be zero.

Another important term is “total variance,” which is utilized for analyzing principal component. In that case, variables are transformed to make its arithmetic mean 0 while variance is 1. Here, “total variance” means summation of all variances of all the under consideration variables.

Since standardized variance equals 1, every variable contributes a part to it. Because of this, total variance is the sum of all variances. If we analyze seven variables, total variance will be 7 [34].

Extracted components perform partition of this variance: 1st component equals 3.2 units of total variance; 2nd matters for 2.1; and it continues until variance is fully accounted for.

Every next component matters for smaller variance; therefore, only initial components are analyzed. After completing this analysis, resulting parts show different correlations but observed variables have no correlation with each other.

Orthogonal versus Oblique Solutions: These solutions will be discussed in principal component analysis that result in orthogonal solutions while in orthogonal solutions; components are not correlated with each other as the term orthogonal means uncorrelated. The solutions, in which, results are in correlated components, are called "oblique solutions." Sometimes, oblique solutions are better because their results are easily interpretable. However, oblique solutions can be complicated to interpret in some situations, and for that, we have discussed interpretation of orthogonal solutions in the current chapter. To learn about oblique solutions, the concepts have good foundation for complicated PCA.

Both procedures are conducted using SAS System's FACTOR process, which provides quite similar outcomes. Factor analysis and PCA have stark similarities.

CHAPTER 6

Predefined PCA plots

6.1 PCA Overview

6.1.1 Scores

It has two-dimensions and a map/scatter plot of scores. The plot provides data regarding the sample patterns. Scores plots (PC1, PC2) help summarizing larger data variation as compared to other pairs [35].

It the samples are closer, they are likely to be similar to each other. Conversely, samples, which have distance, are different. A plot interprets differences and similarities among samples. Figure 6.1 shows an example of PCA Scores plot. As this figure shows, there are three clusters, one cluster on the right, one cluster on the left and one on the middle.

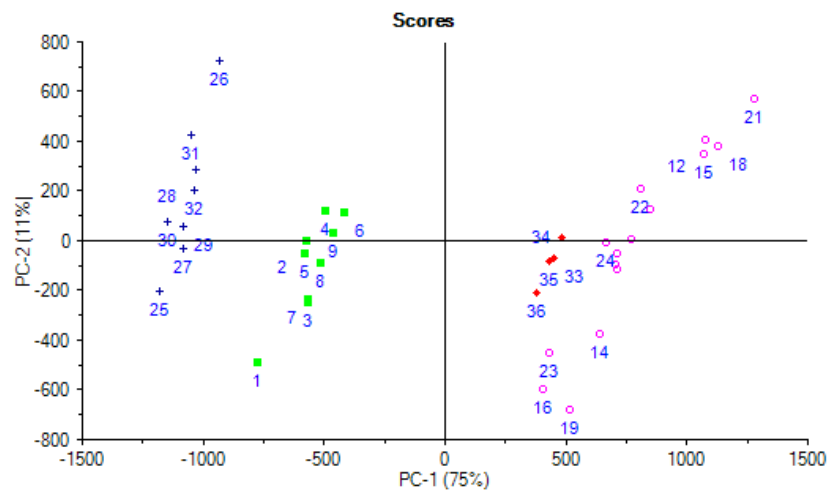


Figure 6.1 Two dimensions and scatter plot of scores[46]

This can help finding out variables causing difference between the samples. Samples located towards right side of the scores plot generally show larger values. We can find the information in a 2D scores plot.

6.1.2 Finding Groups in a Scores Plot

Figure 6.2 exhibits four separate clusters (red, green, pink and blue). Samples within each cluster are similar. Detecting grouping in a scores plot[36].

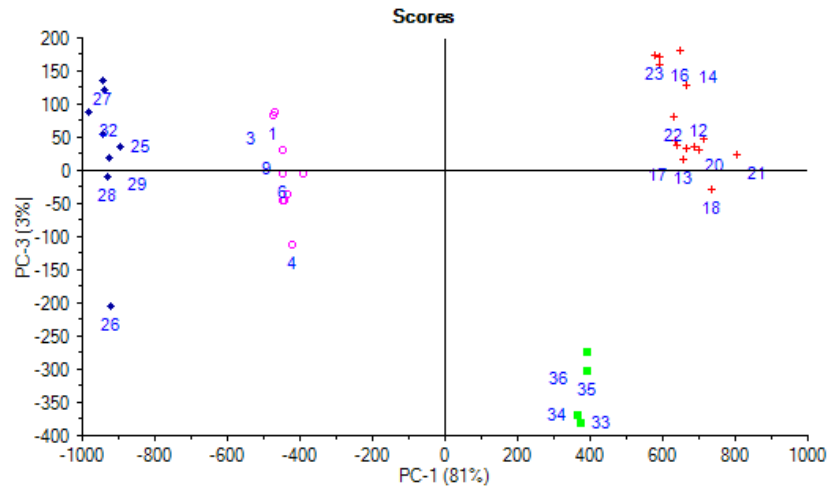


Figure 6. 2 Finding groups in a scores plot [36]

6.1.3 Studying Sample Distribution in Scores Plot

The Scores plot in figure 6.3 shows fan-like layout for majority of samples in the bottom left that later spreads further. The accumulated samples indicate similar properties and vice versa.

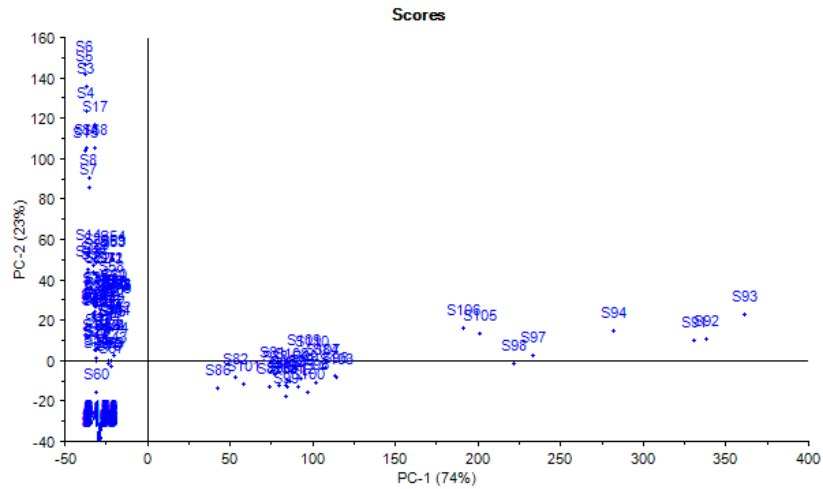


Figure 6.3 shows a situation with four distinct clusters [47]

6.1.4 Calibration and Validation Scores

When the cross and test-set validation methods are used, Unscramble will by default display Calibration and Validation Test scores existing within the same plot. Figure 6.4 shows an example of validation plots where the red dots indicate the validation points.

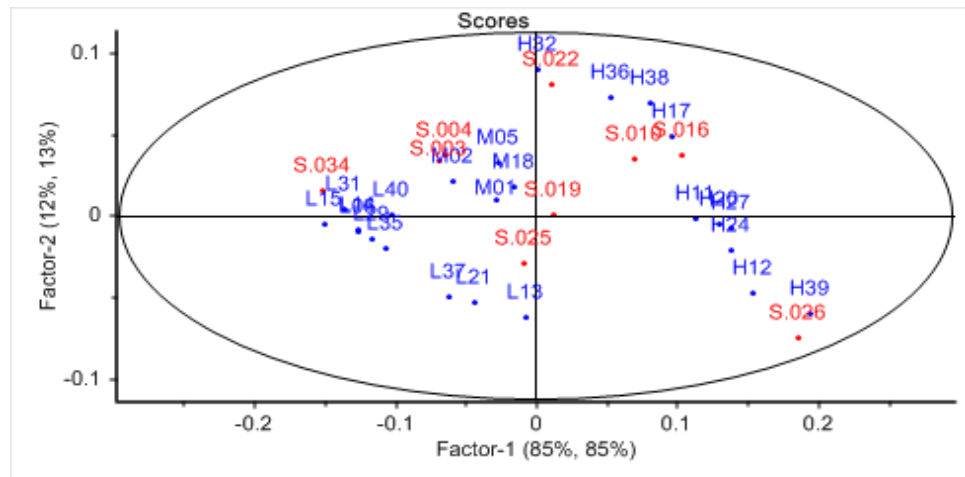


Figure 6.4 Calibration and Validation [48]

6.1.5 Detecting outliers in a scores plot

Outliers should be investigated because they may be part of data collection errors, or there may be inappropriate samples.

Figure 6.5 represents sample-projection in the sub-models, which are utilized for validation, as they can become parts of model or left out. Hence, this plot is only available when any type of cross-validation is chosen. An outlier disturbs the model.

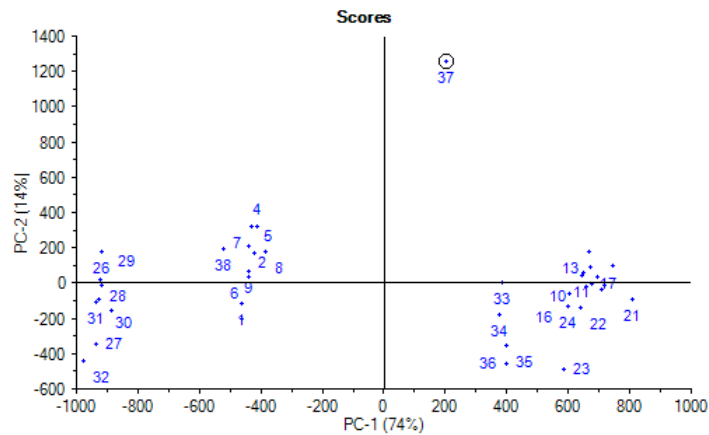


Figure 6.5 Samples shows as outliers [49]

6.2 The Figures Representative

Check extent of variation every component exhibits. This is placed in parentheses next to the axis name. If summation of variances pertaining to two components is more (more than 70%), it provides most of the data, so relationship interpretation has high certainty. If it is smaller, further components/transformations can be possible, or some useful information might exist [37].

Loadings:

A 2D X-loadings scatter plot for two components from PCA has been appropriate for detecting significant variables, which is helpful to interpret component one versus component two, as they show significant changes in X-data. Here, a plot shows significance of two specified variable components. It needs to be utilized with its concerning scores plot. Variables having X-loadings are X-variables, which notmally attains higher values.

Note: Down-weighted variables are displayed in a different colour for easy identification.

6.2.1 X-variables correlation structure

Variables located near on other have higher and positive correlation or if any two components show substantial part of variance of X (figure 6.6). It is also valid for variables existing within the same quadrant. Variables within diagonally-opposite quadrants tend to have negative correlation, which is obvious from the figure, in which, “redness” and “colour” show positive as well as significant correlation. They show negative correlation for thickness. Variables including redness and off-flavour are independent while the correlation between “raspberry flavour” and “off-flavour” is negative.

Some variables such as “sweetness” and "chew resistance" are not possible to interpret because their position is closer to the centre. 12 sensory variable loadings along (PC1, PC2) are given in the diagram:

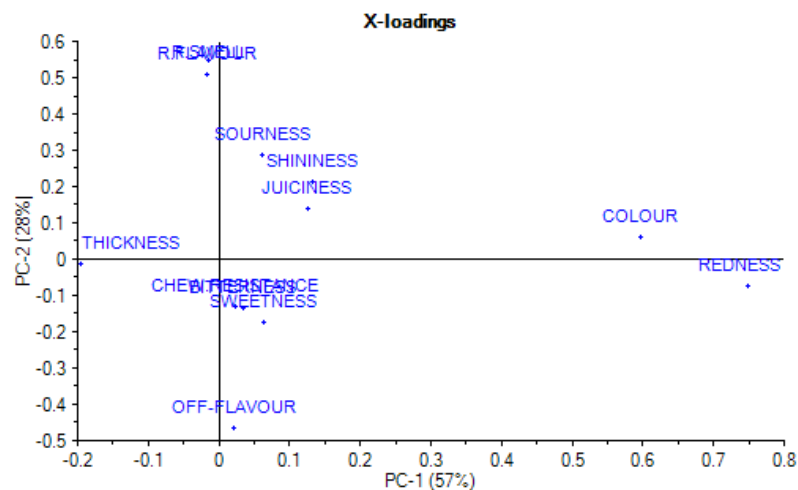


Figure 6.6 Substantial Part of Variance of X [50]

Note: Closer-to-centre variables are poorly exhibited through PCs. We should not make assessment when they are in the plot. While using spectroscopy or time-series, line loadings plot help making interpretations.

That happens when loadings show similar profile and may highlight regions of high importance. Figure 6.7 illustrates the way PCs are overloaded in line-loading plots to finalize components, which can provide information sources. While handling discrete variables, line loadings plots (Figure 6.8) are another option for representing the data[38].

The ascending and descending buttons are fixed to order the loadings according to variables with highest (or lowest) contribution to the PC.

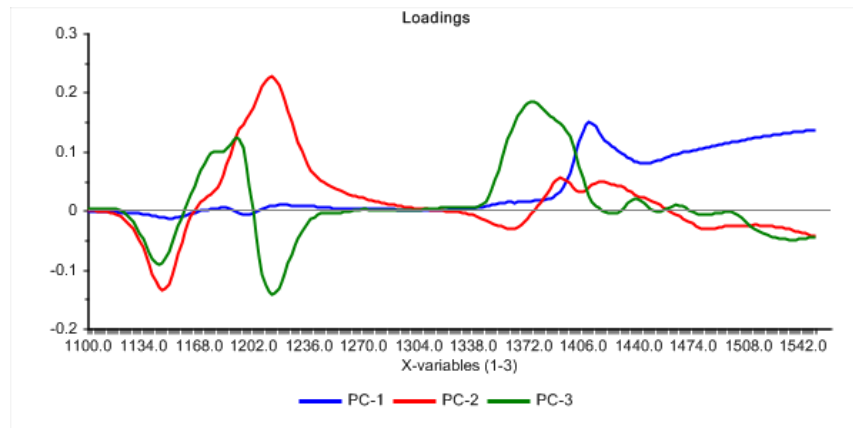


Figure 6.7 Line plot of loadings in ascending order of importance to PC1 [38]

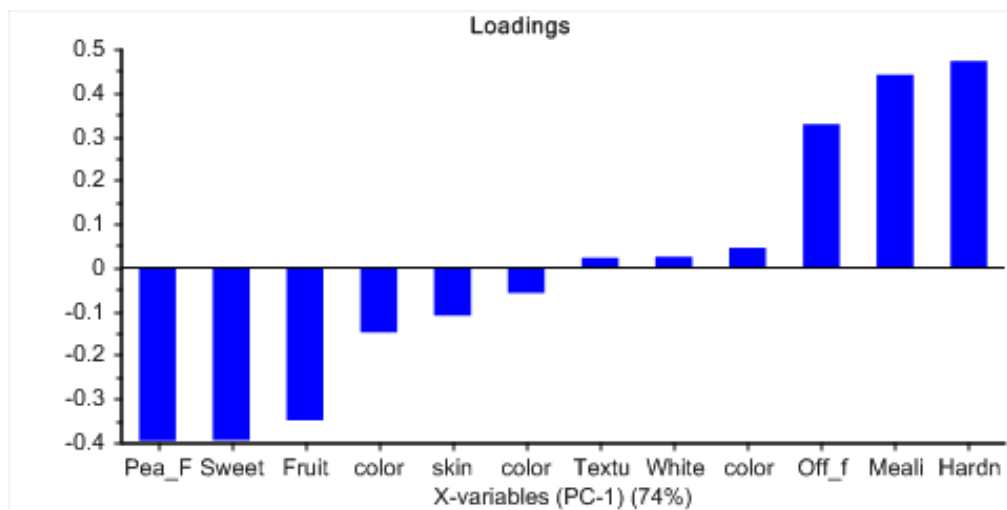


Figure 6.8 shows loading and X-variables[50]

6.3 Correlation Loadings Emphasize Variable Correlations

We use "Correlation Loading" option to discover the structure. They are calculated for every individual variable for given Principal Components as shown in figure 6.9.

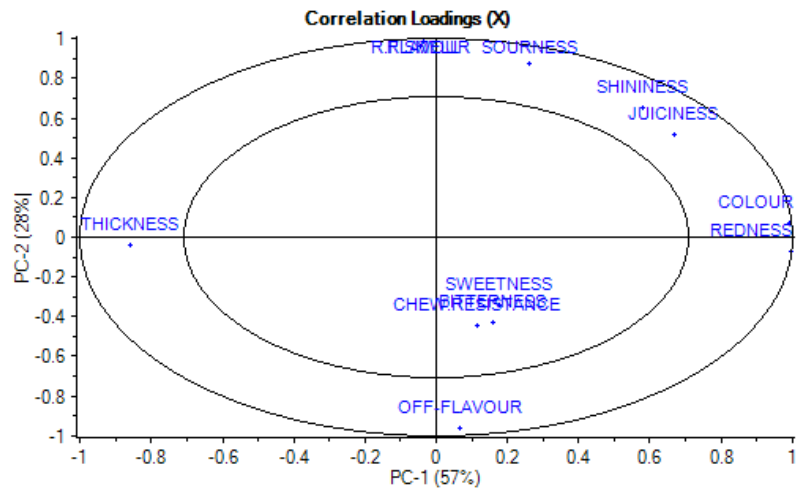


Figure 6.9 Correlation loadings emphasize variable correlation [51]

Correlation loadings (figure 6.10) are also available for 1D line loading plots. Whenever line plot is made, 1D "correlation loadings" toolbar icon will show up. These are good for interpreting significant wavelengths during spectroscopic or contributing variables analysis of time series data. An example is shown below:

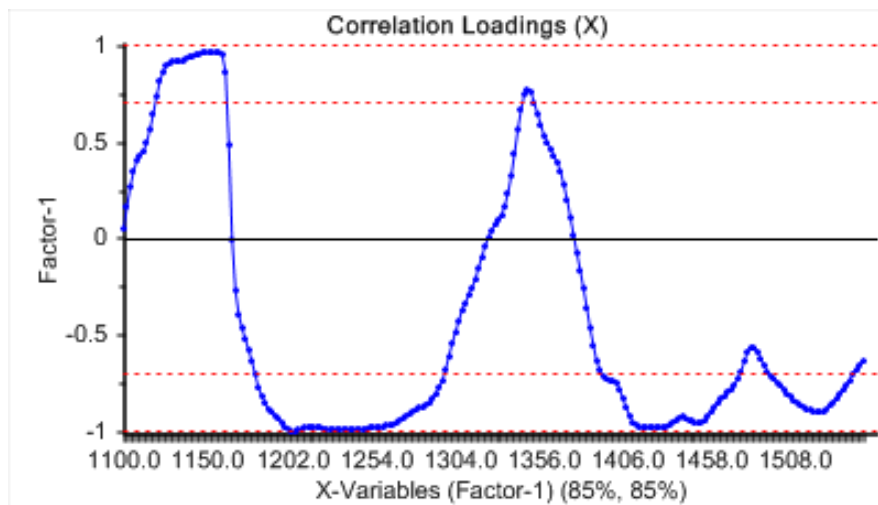


Figure 6.10 Correlation Loading [51]

6.4 Influence Plot

This plot shows the Q- or F- residuals vs. Leverage or Hotel ling's T^2 statistics. They represent two separate types of outliers. The residual statistics on the ordinate axis describe the sample distance to model, whereas the Leverage and Hotel ling's T^2 describe the quality of sample description. Samples having more residual variance, i.e.

located in upper parts of plot, the model poorly describes them including additional components, which might make them better described; however, caution is required that the additional components are predictive and not modelling noise.

As long as the samples with high residual variance are not influential (figure 6.11), it might not be a problem to make them stay in the model as such (the high residual variance may be due to unimportant regions of a spectrum). Samples having more leverage such as those, which are lying towards right of plot, are well described. They are well described because the sample scores may have extreme values for some components in comparison with the remaining samples [39].

Such samples are dangerous in the calibration phase when they get influential to the model. An extreme sample may by itself spans an entire component, which makes the model unreliable. Removal of a highly influential sample will make the model look entirely different and the axes will span altogether different phenomena.

If the variance described is important but unique, one should try to obtain more samples to stabilize the model; otherwise, the sample should be discarded as outlier. Sample having high residual variances and more leverages are the most dangerous outliers. Samples such as these may span up to several components.

Because they also disagree with the majority of the other calibration samples, the model's ability to describe new samples is likely to be poor. The Q- and F- residuals are two different methods for testing the same thing. The F-residuals are available for both calibration and validation other than Q-residuals, which are available for calibration only.

The validated residuals reflect the scheme chosen in the validation and in comparison, it is a bit more conservative assessment of residual outliers. If the residual variance from validation is much higher than what it is for calibration, a researcher should investigate the residuals in more detail. Leverage and Hotelling's T^2 have a difference of only a scaling factor.

The critical limit for Leverage bases on the ad-hoc rule whereas the Hotelling's T^2 critical limit takes student t-distribution.

Influence plot.

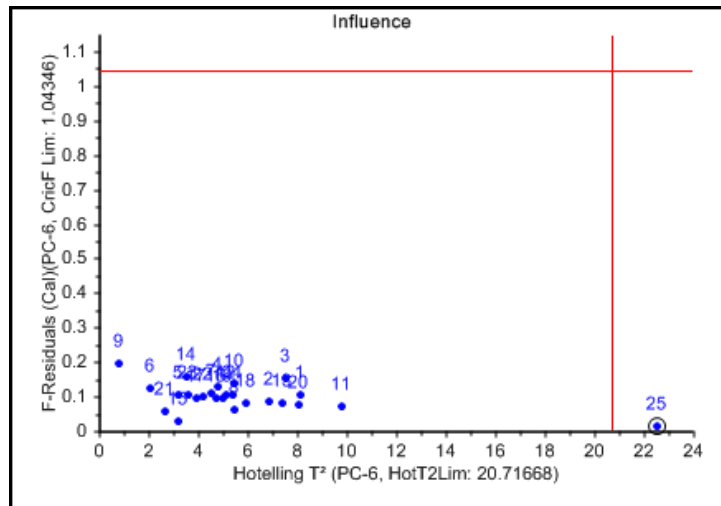


Figure 6.11: Influence plot [52]

In the plot given above, sample 25 creates high-leverage on PC6, which is a dimension of the model. This sample needs checking as a probable outlier. Three cases possibly arise from the influence plot:

Case 1: A sample has more leverage. This is an influential sample. The researcher should check the reasons for it to be influential and decide what to do.

Case 2: A sample possesses high-residual check when variables are poorly described for the sample. It is needed to decide if the sample is an outlier.

Case 3: A sample possesses both high-leverage and a high residual. This sample is most likely an outlier. Retaining this sample is risky.

Note: While using designed data, every sample's leverage can be understood by construction, and their leverages are optimum, i.e. design samples have similar contributions for a model. So, the researcher should not take leverages too seriously while conducting a regression analysis.

Now the question is How to deal with an influential sample? We should comprehend why samples have more leverage. We can take basic data and check it in comparison with original recording. Two cases should be considered:

Case 1: If any error exists in the data, a researcher should correct it because if true values are not found, the experiment cannot be redone to obtain real values, we should consider erroneous values as missing.

Case 2: Errors do not exist unless a different sample exists, for example, extreme variable values. It must be checked whether that particular sample is required or irrelevant.

First case scenario is that the researcher should test more samples and focus on the most feasible ones. Second case is removing high-leveraged sample. Calibration and validation of samples should be exhibited in the influence plot by toggling between them using the "and" button. This is only possible if the chosen validation method is cross validated or has test set validation.

6.5 Explained/Residual Variance

This plot shows as to how much data variation as the total residual variance is summation of residual squares of variables divided by the "degree of freedom."

Total explained variance= $100 * (\text{initial} - \text{residual variance}) / (\text{initial variance})$, which is proportional to the original variance. Both variances can be computed after data components 0, 1, 2 etcetera.

Models with little total residual variance or maximum, the explained variance explain variation in X, which is shown in the example below. Ideally, we need simple models, where residual variance approaches 0 having fewer components. Calibration variance depends on the model's calibration data [40], which is not utilized for building the model. Then we match both variances. If they differ significantly, there arises a significant question whether the obtained information actually represents the target information. Figure 2 illustrates that the residual validation variance was greater as compared to the residual calibration variance.

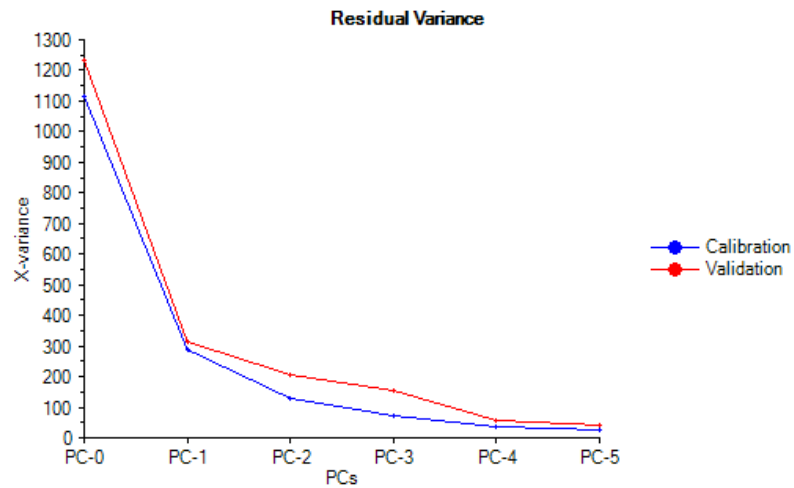


Figure 6.12 shows data variation

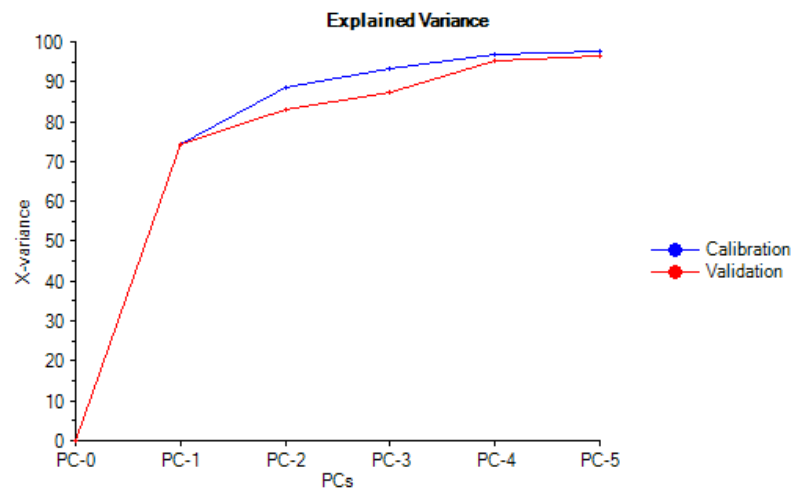


Figure 6.13 shows data variation

This shows that the calibration data were appropriate but the model did not appropriately describe the new data. On the contrary if the two residual variance curves are close together, the model is representative. Here, the calibration and validation data indicates the existence of outliers.

Outlier causes explained variance during validation.

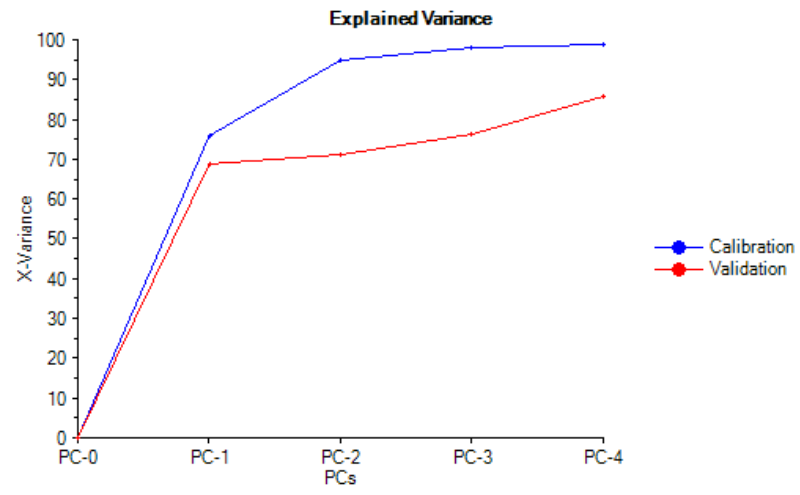


Figure 6.14 shows variances

RESULTS AND DISSCUSSIONS

7.3 Signals to Noise Ratio

We performed the LIBS measurements for many tablets to find signal noise ratio [43] but we chose the best two tablets Brufen and Glucosamine.

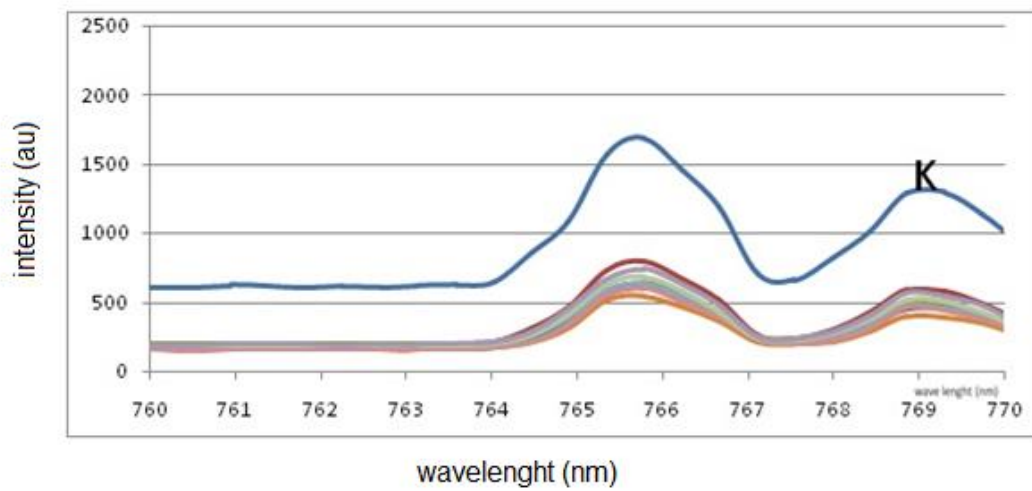
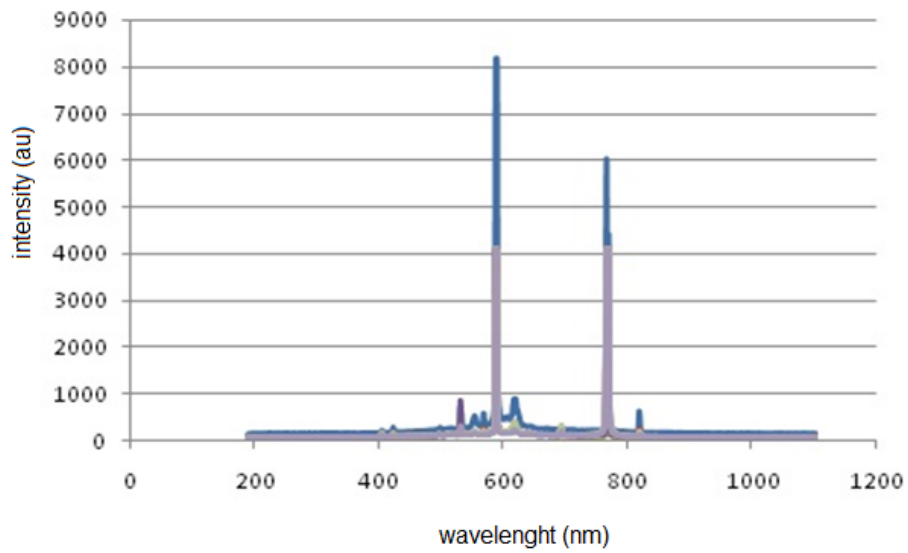
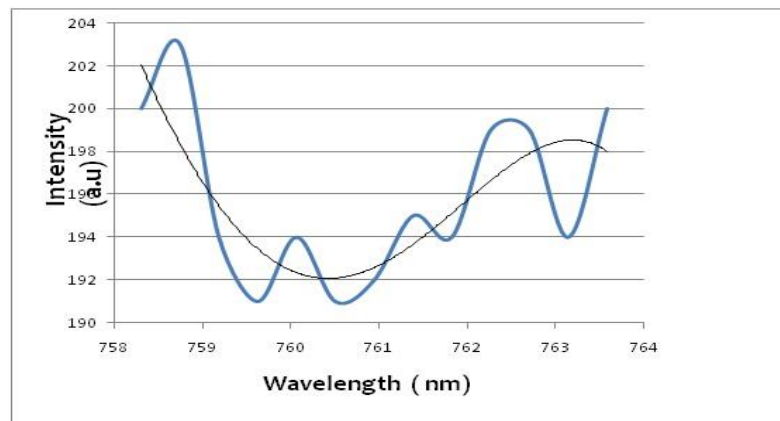


Figure 7.4 shows signals to noise ratio of K



Error	1.76
S/N for Na	87.63

Figure 7.5: Signal to Noise ratio glucoamine for Na



Error	2.45
S/N for K	274.34

Figure 7.6: signal to noise ratio brufin

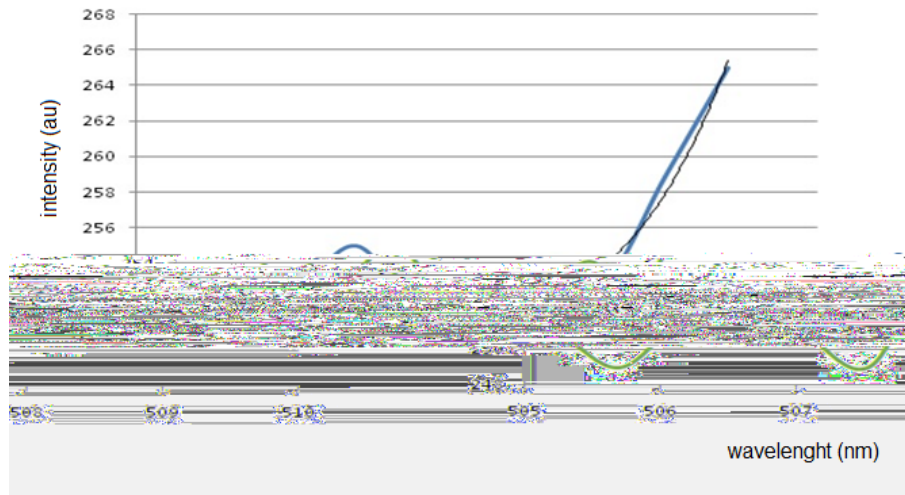


Figure 7.7: Signal to noise ratio glucoamine for Na

7.4 Spectral Analysis

LIBS representative spectrum pertaining to three drug samples is plotted separately in Fig. 2 for the sake of clarity. The analysis took place for elements including carbon, nitrogen, hydrogen and oxygen, which are primary components in the tablets. having organic ingredients as well. Basic Aferine components do not have no nitrogen but the LIBS shows nitrogenous peaks. This might have happened because of presence of nitrogen in Aferine flavouring or colouring. The spectrum shows presence of iron, sodium, magnesium, titanium and calcium.

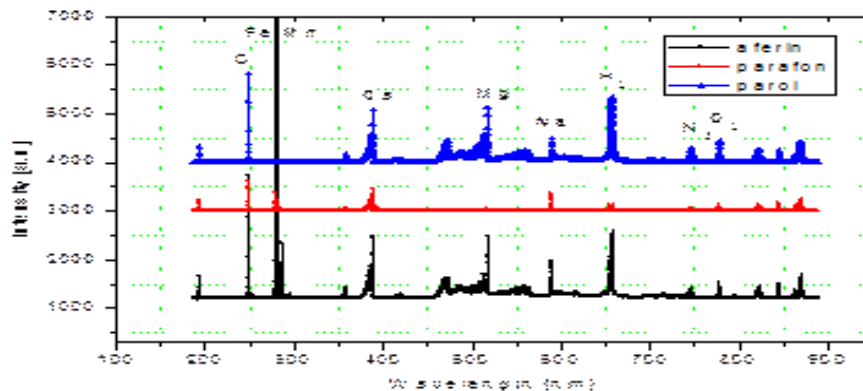


Figure 7.8 LIBS spectra for the studied samples (a) Aferin, (b) Parafon, (c) Parol

We think that other metals could be recipients (Brunette et al., 2001) (especially sodium) or contaminants [44]. Recordings show nitrogen, carbon, oxygen and hydrogen, so, coated tablets had considerable titanium. Table 2 shows spectra elements and their concerned emission wavelengths.

Table 7.2: Different peaks were found in LIBS spectra, which showed significant atomic elements.

S. No.	Element	Wavelength (nm)
1	Carbon	247.85
2	Iron	279.78, 283.59, 285.18
3	Manganese	279.10, 279.48, 380.96
4	Sodium	589.0, 589.60
5	Vanadium	251.16, 572.68, 635.70
6	Oxygen	777.19, 777.41, 777.53, 822.18, 822.76
7	Nitrogen	742.36, 744.23, 746.83, 818.48, 818.80, 821.63, 824.23
8	Hydrogen	656.27
9	Magnesium	518.36
10	Titanium	394.8, 395.6, 395.8, 399.8
11	Calcium	393.37, 396.86

7.5 Ratio Metric Analysis

We explored ratio-metric approach for analyzing tablet contents through oxygen-to-nitrogen intensity ratios. Previously, it has been a useful approach for nitro-compound identification, namely 4-nitroaniline and 4-nitrotoluene [45]. The oxygen peaks on 777nm . Figure (3) shows that nitrogen peaks on 742.36nm (for N1) and 744.23 nm (for N2). Figures 3 and 4 help evaluating O/N ratio.

LIBS spectra has been unable to fully resolve the oxygen peak.

Figure 3: Oxygen LIBS peaks from (a) Aferin, (b) Parafon, (c) Parol

The dots show experimental points.

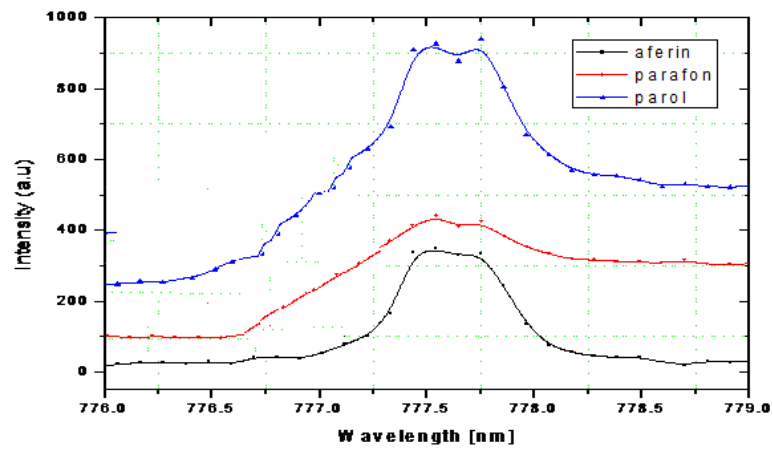


Figure 7. 9 Oxygen LIBS peaks from (a) Aferin, (b) Parafon, (c) Parol. The dots indicate experimental points.

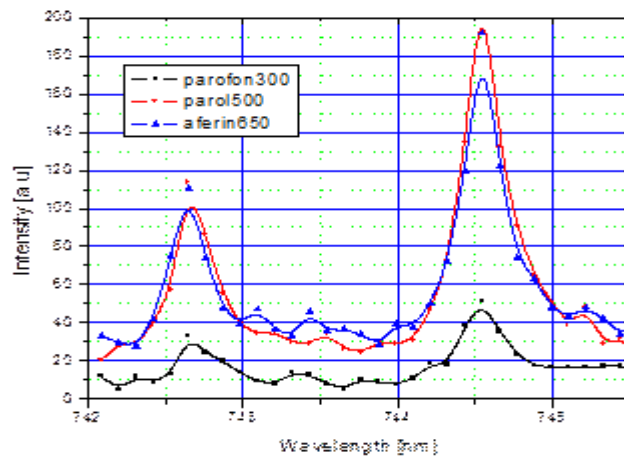


Figure 7. 10 Nitrogen (N1 and N2) LIBS peaks from (a) Aferin, (b) Parafon, (c) Parol. The dots show experimental points

Two O/N ratios were found through direct evaluation of O/N intensity ratios using areas under peaks, which result in extreme values mentioned in Table 3.

Table 7. 3 Oxygen/nitrogen ratios at oxygen peak 777 nm (O), nitrogen peaks at 742.36 nm for N1 and 744.23 nm for N2.

	Sample name	O/N ₁	O/N ₂
1	aferin1_500mg	4.25	2.55
2	parofon_500mg	41.08	27.85
3	Parol_500mg	23.05	12.5

Density of states calculated for the three tablets for the hydrogen peak at 656.65 nm (Figure.5) considering plasma temperature $c=10000$ K. Figure 6 shows the values of density of states for different tablets under consideration. Figure 5 shows H2 peaks for the sample tablets. Figure 6 shows the density of states of different tablets. 21×10^4

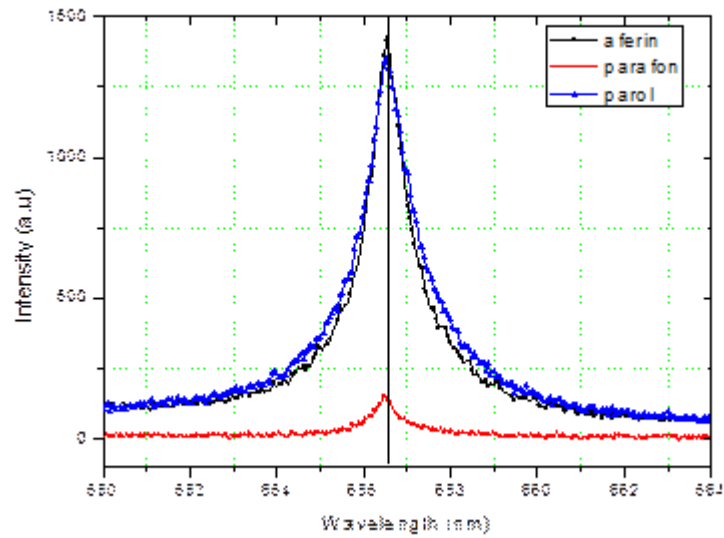


Figure 7. 11 shows the position of H2 peaks for the different tablets.

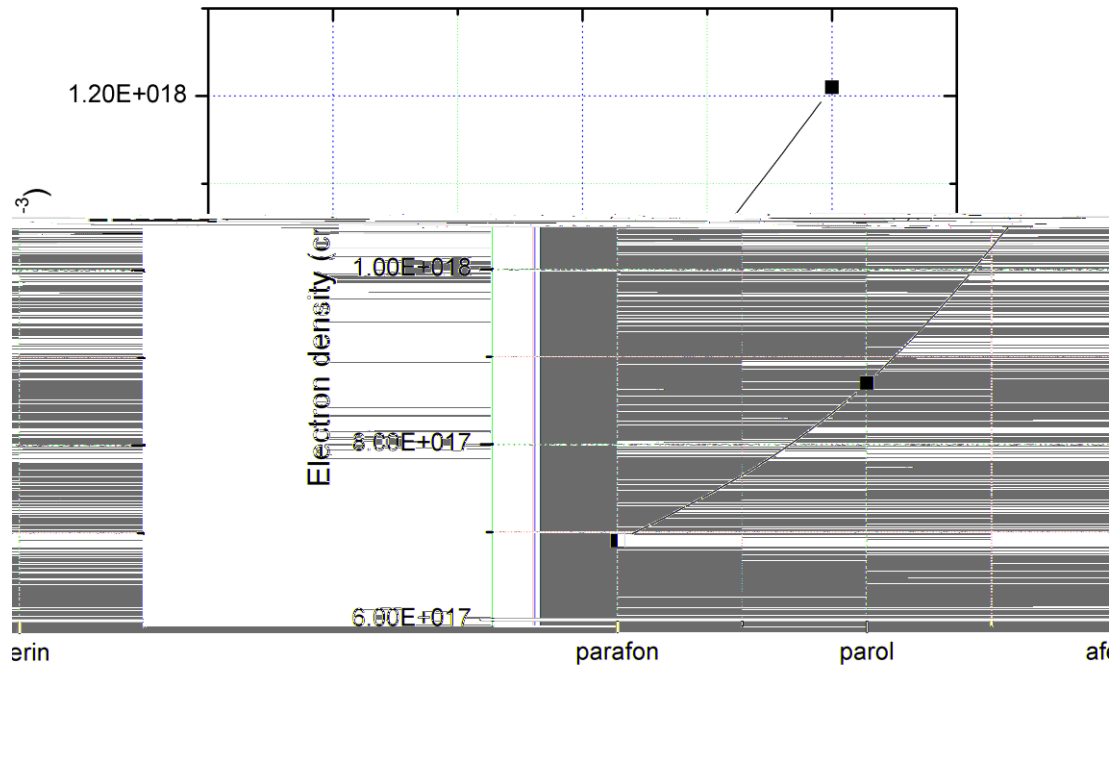


Figure 7.12 shows the density of states of different tablets.

7.6 Loadings

The 2D X-loadings scatter plot having two PCA components helps detecting significant variables, and that also helps interpreting both the components in comparison with each other because they have greatest differences in the X-data. The plot illustrates the significance of some variables for both the components

7.6.1 X-variables correlation structure

Variables, which are located closer to each other on a loadings plot, have significant and positive correlation value. The variables located near the centre have been inappropriately explained by PCs. The researcher should not interpret those variables in a plot because spectroscopic/time series based loadings plots provide better interpretation mainly because those loadings have a profile, which is quite similar as compared to the original data highlighting important areas.

Case 1: A sample has a high leverage.

This is an influential sample. Reasons should be checked for it to be influential for deciding what to do.

Case 2: A sample has a high residual.

It needs to be checked which variables are poorly described by the model for this sample for deciding if this sample is an outlier.

Case 3: A sample is a high-leverage and high-residual sample. This sample is most likely an outlier. Retaining this sample in the model is risky.

7.7 Software Analysis

We applied software on tablet Aferin (500mg) as shown in the figure below:

We used unscramble software this program depends on:

- Application knowledge (table) 40%
- Common sense 30%
- Statistics 20%
- Mathematical 10%

7.8 Correlation and variance analysis

As shown in the figure Aaferin 650 mg. There is error, which is well explained as other variables link of error, which is proportional to how much percentage is exactly explained.

Correlation between the two variables ParolParol 500mg and Parafon 300mg indicates that they need to be close to each other and so, PCA is very well explained in this case.

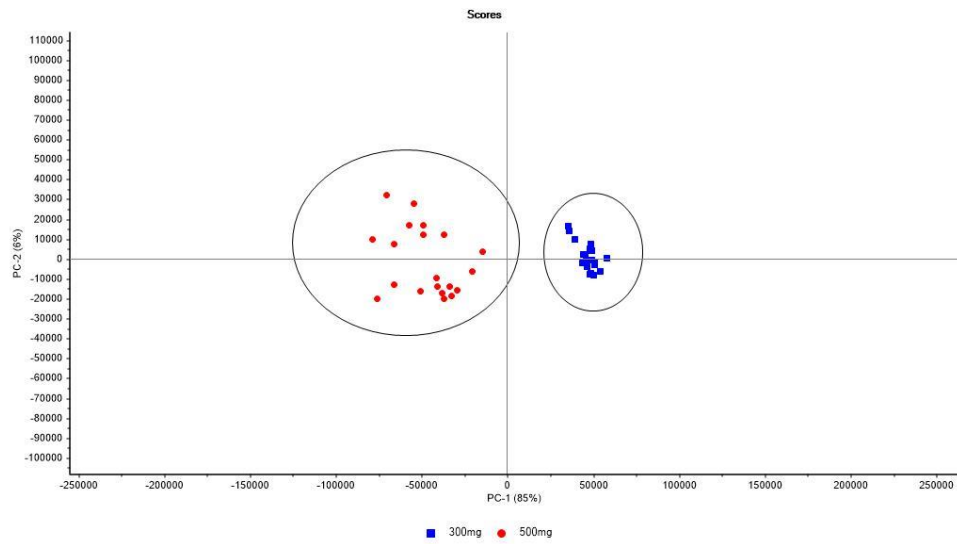


Figure 7. 13 PCA graph shows two components Parafon 300mg and Parol 650 mg

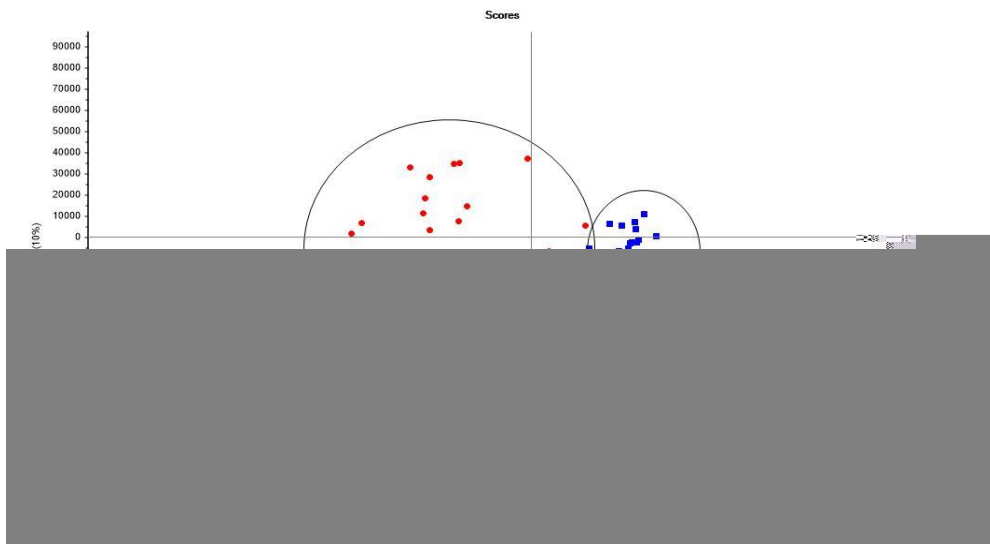


Figure 7. 14 PCA graph shows two components Aferin 650 mg and Parafon 300mg

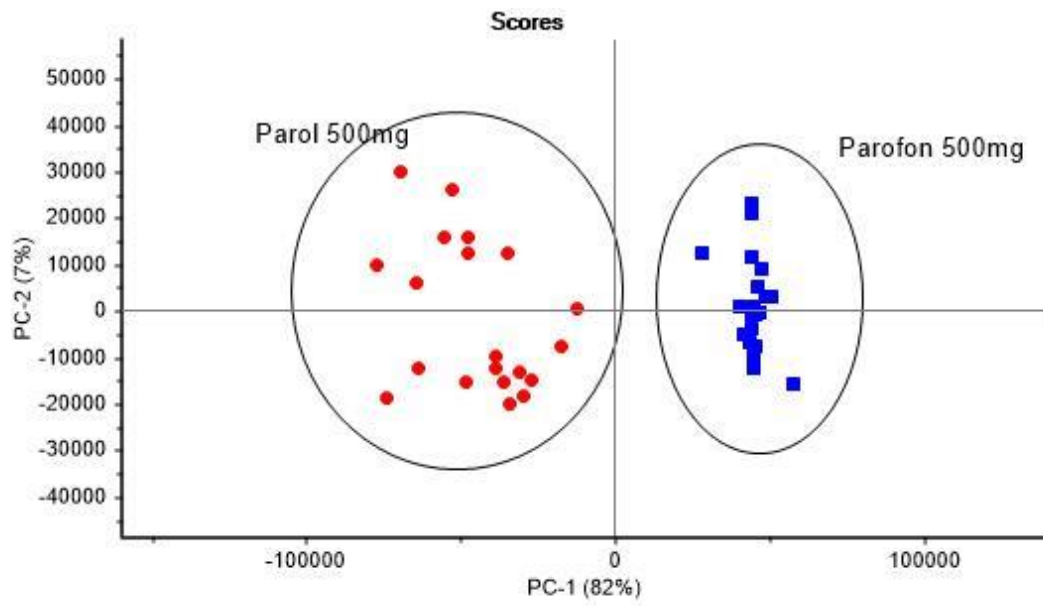


Figure 7.17 PCA graph shows two components Parol 500 mg and parofon 500 mg.

Conclusion

This study was conducted to comprehend those physical processes, which help investigation of pharmaceutical drugs and medicines by laser-induced plasma (breakdown) spectroscopy.

LIBS signals of different samples were analysed and the standard deviations as well as the experimental uncertainties were determined. The plasma emission spectra helps us study the temporal density of electrons in plasma when expansionary and decaying is under process. In this study, we used ratio-metric approach for identifying the tablets based on respective oxygen-to-nitrogen intensity ratio values. The oxygen peaks at 777nm while nitrogen peaks at 742.36nm for N1 and 744.23 nm for N2, which were used for evaluating the oxygen to nitrogen (O/N) ratios. We found two O/N. A direct O/N intensity ratio evaluations was done when we considered areas underneath the peaks, which resulted in significant values. On the other hand, electron density of states calculated for the three tablets for the hydrogen peak was at 656.65nm (Plasma temperature 10000 K).

As a part of our thesis, we have evaluated LIBS as a quick and direct process to analyze drug content. Most of the tablet contents were organic but still a significant fraction of chemicals was found to be very different as compared to other tablet components. Qualitative analyses have been conducted to distinguish tablets from each other. Drug content measurement can, therefore, be conducted by quantifying this element.

LIBS can provide new surface and internal information of pharmaceutical materials, which is useful for pharmaceutical solid dosage preparation. The technology needs no sample preparation, takes very less time approximately less than one minute, it is element-specific, contained in the chemical structure of drugs, and/or other functional materials.

Qualitative and quantitative determinations can then be obtained rapidly on drug formulations during the developmental stage or commercial manufacturing. In this work, we analysed the effectiveness of LIBS as a routine monitoring technique for commercial pharmaceutical tablets such as Parofon 300 mg, Parol 500 mg and Aferine 650 mg. We checked their composition and discriminated them with other drugs when

we purchased them without prescription from a local pharmacy because their over-the-counter sale is legal. We conducted PCA analysis for qualitatively in order to distinguish the tablets as seen in the Figure 7.17. Based on the LIBS spectra and the calculated physical parameters, LIBS technique shows a successful differentiation between the different types of pharmaceutical tablets. The combination of chemometric techniques such as PCA with the LIBS shows a very successful classification of the tablets from each other.

Finally, the results show that the LIBS with PCA is an easy, cost effective, and accurate technique than some others traditional analysis techniques for pharmaceutical tablets.

REFERNCES

1. Anabitarte, F., A. Cobo, and J.M. Lopez-Higuera, *Laser-Induced Breakdown Spectroscopy: Fundamentals, Applications, and Challenges*. ISRN Spectroscopy, 2012. 2012: p. 12.
2. Archambault, J.-F., A. Vintiloù, and E. Kwong, *The effects of physical parameters on laser-induced breakdown spectroscopy analysis of intact tablets*. AAPS PharmSciTech, 2005. 6(2): p. E253-E261.
3. De Lucia Jr, F.C., et al., *Multivariate analysis of standoff laser-induced breakdown spectroscopy spectra for classification of explosive-containing residues*. Applied optics, 2008. 47(31): p. G112-G121.
4. Evans, E.H., et al., *Advances in atomic emission, absorption and fluorescence spectrometry and related techniques*. Journal of Analytical Atomic Spectrometry, 2002. 17(6): p. 622-651.
5. Hassoun, M.H., *Fundamentals of artificial neural networks*. 1995: MIT press.
6. Snyder, E.G., et al., *Laser-induced breakdown spectroscopy for the classification of unknown powders*. Applied optics, 2008. 47(31): p. G80-G87.
7. Demtröder, W., *Laser spectroscopy: basic concepts and instrumentation*. 2013: Springer Science & Business Media.
8. Corney, A., *Atomic and laser spectroscopy*. 1978: Clarendon Press Oxford.
9. Margulies, S. and J. Ehrman, *Transmission and line broadening of resonance radiation incident on a resonance absorber*. Nuclear Instruments and Methods, 1961. 12: p. 131-137.
10. Everitt, B.S., *An R and S-PLUS® companion to multivariate analysis*. 2006: Springer Science & Business Media.
11. Jolliffe, I.T., *Principal component analysis and factor analysis*. Principal component analysis, 2002: p. 150-166.

12. Niu, H. and R. Houk, *Fundamental aspects of ion extraction in inductively coupled plasma mass spectrometry*. Spectrochimica Acta Part B: Atomic Spectroscopy, 1996. 51(8): p. 779-815.
13. Hybl, J.D., G.A. Lithgow, and S.G. Buckley, *Laser-induced breakdown spectroscopy detection and classification of biological aerosols*. Applied spectroscopy, 2003. 57(10): p. 1207-1215.
14. Thomas, R., *Emerging Technology Trends in Atomic Spectroscopy Are Solving Real-World Application Problems*. Spectroscopy, 2014. 29: p. 42-51.
15. Scoutaris, N., S. Ross, and D. Douroumis, *Current trends on medical and pharmaceutical applications of inkjet printing technology*. Pharmaceutical research, 2016. 33(8): p. 1799-1816.
16. Myakalwar, A.K., et al., *Laser-induced breakdown spectroscopy-based investigation and classification of pharmaceutical tablets using multivariate chemometric analysis*. Talanta, 2011. 87: p. 53-59.
17. Rusak, D., et al., *Fundamentals and applications of laser-induced breakdown spectroscopy*. Critical Reviews in Analytical Chemistry, 1997. 27(4): p. 257-290.
18. Raja, M.Y.A., et al., *Resonant periodic gain surface-emitting semiconductor lasers*. IEEE Journal of Quantum Electronics, 1989. 25(6): p. 1500-1512.
19. Chylek, P., et al., *Pressure dependence of the laser-induced breakdown thresholds of gases and droplets*. Applied optics, 1990. 29(15): p. 2303-2306.
20. Rosen, D. and G. Weyl, *Laser-induced breakdown in nitrogen and the rare gases at 0.53 and 0.357 μm* . Journal of Physics D: Applied Physics, 1987. 20(10): p. 1264.
21. Skogerboe, R., I. Urasa, and G. Coleman, *Characterization of a DC plasma as an excitation source for multielement analysis*. Applied Spectroscopy, 1976. 30(5): p. 500-504.

22. Cwiertny, D.M., et al., *Environmental designer drugs: when transformation may not eliminate risk*. 2014, ACS Publications.
23. Kurniawan, H., et al., *Detection of density jump in laser-induced shock wave plasma using a rainbow refractometer*. *Applied Spectroscopy*, 2001. 55(1): p. 92-97.
24. Lo, C., *The Detection of Gravitational Wave with the Laser Interferometer*. 2005.
25. Doucet, F.R., et al., *Quantitative molecular analysis with molecular bands emission using laser-induced breakdown spectroscopy and chemometrics*. *Journal of Analytical Atomic Spectrometry*, 2008. 23(5): p. 694-701.
26. Boxall, A.B., et al., *Pharmaceuticals and personal care products in the environment: what are the big questions?* *Environmental health perspectives*, 2012. 120(9): p. 1221.
27. Swarbrick, B., *Process analytical technology: A strategy for keeping manufacturing viable in Australia*. *Vibrational spectroscopy*, 2007. 44(1): p. 171-178.
28. Vadillo, J.M. and J.J. Laserna, *Laser-induced plasma spectrometry: truly a surface analytical tool*. *Spectrochimica Acta Part B: Atomic Spectroscopy*, 2004. 59(2): p. 147-161.
29. Gornushkin, I., et al., *Microchip laser-induced breakdown spectroscopy: a preliminary feasibility investigation*. *Applied spectroscopy*, 2004. 58(7): p. 762-769.
30. Fortes, F.J., et al., *Laser-induced breakdown spectroscopy*. *Analytical chemistry*, 2012. 85(2): p. 640-669.
31. Bramble, S., et al., *Ultraviolet luminescence from latent fingerprints*. *Forensic science international*, 1993. 59(1): p. 3-14.
32. Everitt, B.S., *Multivariable modeling and multivariate analysis for the behavioral sciences*. 2009: CRC Press.

33. Maćkiewicz, A. and W. Ratajczak, *Principal components analysis (PCA)*. Computers & Geosciences, 1993. 19(3): p. 303-342.
34. Ringnér, M., *What is principal component analysis?* Nature biotechnology, 2008. 26(3): p. 303-304.
35. Abdi, H. and L.J. Williams, *Principal component analysis*. Wiley interdisciplinary reviews: computational statistics, 2010. 2(4): p. 433-459.
36. Clarke, K. and R. Warwick, *An approach to statistical analysis and interpretation*. Change in marine communities, 1994. 2.
37. Peres-Neto, P.R., D.A. Jackson, and K.M. Somers, *Giving meaningful interpretation to ordination axes: assessing loading significance in principal component analysis*. Ecology, 2003. 84(9): p. 2347-2363.
38. Wold, S., K. Esbensen, and P. Geladi, *Principal component analysis*. Chemometrics and intelligent laboratory systems, 1987. 2(1-3): p. 37-52.
39. Bro, R. and A.K. Smilde, *Principal component analysis*. Analytical Methods, 2014. 6(9): p. 2812-2831.
40. Sargent, R.G. *Verification and validation of simulation models*. in *Proceedings of the 37th conference on Winter simulation*. 2005. winter simulation conference.
41. Harmon, R.S., R.E. Russo, and R.R. Hark, *Applications of laser-induced breakdown spectroscopy for geochemical and environmental analysis: A comprehensive review*. Spectrochimica Acta Part B: Atomic Spectroscopy, 2013. 87: p. 11-26.
42. Missaghi, S. and R. Fassihi, *A novel approach in the assessment of polymeric film formation and film adhesion on different pharmaceutical solid substrates*. AAPS PharmSciTech, 2004. 5(2): p. 32-39.
43. Johnson, D.H., *Signal-to-noise ratio*. Scholarpedia, 2006. 1(12): p. 2088.

44. Ahrens, V., et al., *Sub-Doppler Saturation Spectroscopy of HCN up to 1 THz and Detection of $J= 3 \rightarrow 2$ ($4 \rightarrow 3$) Emission from TMC1*. *Zeitschrift für Naturforschung A*, 2002. 57(8): p. 669-681.
45. Rai, P.K., et al., *Glycemic properties of Trichosanthes dioica leaves*. *Pharmaceutical biology*, 2008. 46(12): p. 894-899.
46. P. Taylor, "Critical Reviews in Analytical Chemistry Fundamentals and Applications of Laser-Induced Breakdown Spectroscopy Fundamentals and Applications of Laser-Induced Breakdown Spectroscopy," *Crit. Rev. Anal. Chem.*, no. March 2012, pp. 37–41, 2006.
47. D. A. Rusak, B. C. Castle, B. W. Smith, and J. D. Winefordner, "Fundamentals and Applications of Laser-Induced Breakdown Spectroscopy," *Critical Reviews in Analytical Chemistry*, vol. 27, no. 4. pp. 257–290, 1997.
48. A. A. Van Dijk, L. L. Van Wijk, A. Van Vliet, P. Haris, E. Van Swieten, G. I. Tesser, and G. T. Robillard, "Structure characterization of the central repetitive domain of high molecular weight gluten proteins. I. Model studies using cyclic and linear peptides," *Protein Sci.*, vol. 6, no. 3, pp. 637–648, 1997.
49. T. S. I. Incorporated, "Pharmaceutical Ingredient Uniformity Determination Using Libs," no. Table 1, pp. 1–3.
50. J.-F. Archambault, A. Vintiloù, and E. Kwong, "The effects of physical parameters on laser-induced breakdown spectroscopy analysis of intact tablets," *AAPS PharmSciTech*, vol. 6, no. 2, pp. E253–E261, 2005.
51. A. K. Myakalwar, S. Sreedhar, I. Barman, N. C. Dingari, S. Venugopal Rao, P. Prem Kiran, S. P. Tewari, and G. Manoj Kumar, "Laser-induced breakdown spectroscopy-based investigation and classification of pharmaceutical tablets using multivariate chemometric analysis.," *Talanta*, vol. 87, pp. 53–9, Dec. 2011.
52. "Principal Component Analysis | I.T. Jolliffe | Springer." [Online]. Available: <https://www.springer.com/us/book/9780387954424>.